AD-A161 131 RE-EVALUATION OF SURFACE PROPERTIES OF OXIDE-CATHODE MATERIALS(U) UNIVERSITY COLL CORK (IRELAND) DEPT OF CHEMISTRY J CUNNINGHAM 15 JUL 85 AFOSR-TR-85-0933 1/1

UNCLASSIFIED AFOSR-84-0129 F/G 7/4 NL

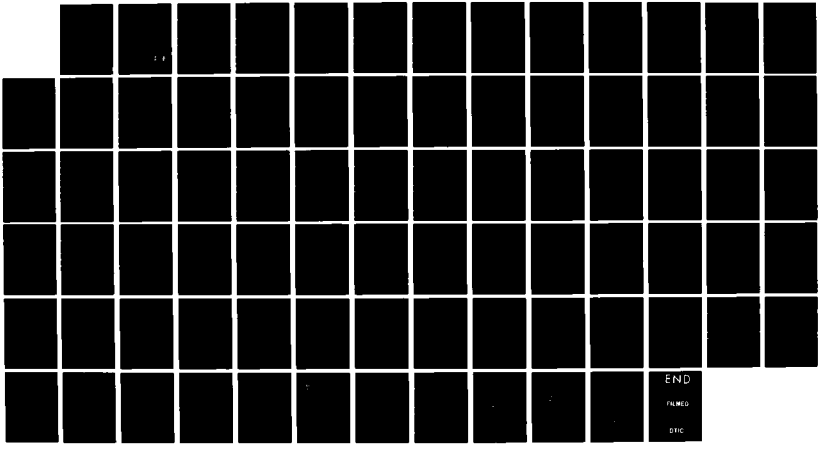

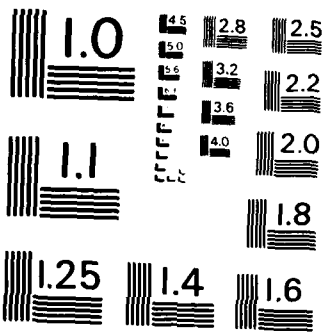

MICROCOPY RESOLUTION TEST CHART
NATIONAL BUREAU OF STANDARDS - 1963 - A

(2)

Grant Number : AFOSR-84-0129

RE-EVALUATION OF SURFACE PROPERTIES OF OXIDE CATHODE MATERIALS

Professor Joseph Cunningham
Physical Chemistry Laboratories
University College Cork
Cork Ireland

15 July, 1985

Final Report, 01 Jul. 1984 - 28 Feb. 1985

Approved for public release; distribution unlimited

Prepared for EOARD, 223/231 Old Marylebone Road, London NW1 5TH.

SECURITY CLASSIFICATION OF THIS PAGE (When Data Entered) UNCLASSIFIED

REPORT DOCUMENTATION PAGE	READ INSTRUCTIONS BEFORE COMPLETING FORM
1. REPORT NUMBER AFOSR-TR- 85-0933	2. GOVT ACCESSION NO. AD-A161131 / 3. RECIPIENT'S CATALOG NUMBER
4. TITLE (and Subtitle) Re-Evaluation of Surface Properties of Oxide-Cathode Materials	5. TYPE OF REPORT & PERIOD COVERED Final Report 01 Jul. 1984-28 Feb. 1985
	6. PERFORMING ORG. REPORT NUMBER
7. AUTHOR(s) Joseph Cunningham Physical Chemistry Laboratories	8. CONTRACT OR GRANT NUMBER(s) AFOSR-84-0129
9. PERFORMING ORGANIZATION NAME AND ADDRESS Chemistry Department University College Cork Cork Ireland	10. PROGRAM ELEMENT, PROJECT, TASK AREA & WORK UNIT NUMBERS PE-6 102F Project-Task 2301/D1
11. CONTROLLING OFFICE NAME AND ADDRESS AFOSR/~~PKZ~~ NC Building 410 Bolling AFB DC 20332	12. REPORT DATE 15 July, 1985
	13. NUMBER OF PAGES
14. MONITORING AGENCY NAME & ADDRESS(if different from Controlling Office)	15. SECURITY CLASS. (of this report) UNCLASSIFIED
	15a. DECLASSIFICATION/DOWNGRADING SCHEDULE

16. DISTRIBUTION STATEMENT (of this Report)

Approved for Public Release : Distribution Unlimited

17. DISTRIBUTION STATEMENT (of the abstract entered in Block 20, if different from Report)

Approved for Public Release : Distribution Unlimited

18. SUPPLEMENTARY NOTES

19. KEY WORDS (Continue on reverse side if necessary and identify by block number)

Alkaline Earth Oxides : MgO; CaO; SrO; BaO
Surface Doped Oxides : BaO/MgO; BaO/SrO; CaO/MgO
Surface Reconstruction (Rumpling)
Surface Luminescence : Surface Catalytic Activity.

20. ABSTRACT Surface properties of high-surface-area samples of alkaline earth oxides BaO, MgO, SrO and CaO - prepared singly as pure materials or as binary systems having BaO dispersed onto the surface of another of the oxides - have been examined using as probes the luminescence and the catalytic activity of the materials. Comparisons of results from the pure systems with those from the binary systems are consistent with extensive reconstruction (rumpling) of the surface layers of the surface-doped binary systems. Such rumpling can produce up to one half of a monolayer of surface ions jutting out from the surface with a high degree of coordinative unsaturation and resultant high lability and catalytic activity.

DD FORM 1 JAN 73 1473 EDITION OF 1 NOV 65 IS OBSOLETE

UNCLASSIFIED
SECURITY CLASSIFICATION OF THIS PAGE (When Data Entered)

PREFACE

Emphasis in much of the published research on the major constituents of oxide-cathodes, - viz. BaO and SrO or CaO produced as high surface area materials by decomposition of mixtures of the corresponding carbonates - has been placed upon modifications of work-function and other surface properties brought about by small coverages of the mixed-oxide surface with metallic barium. Relatively little attention has been given *EITHER* to the surface-structure of the mixed oxides themselves, *OR* to the possibility that strongly-modified surface structures of such oxides may also contribute very significantly to efficient thermionic emission and low work function, as obtained with mixed-oxide-cathodes rather than with single pure oxides. The work undertaken under this minimally-funded effort concentrated upon the former of the two interesting points, viz. the surface structure of the mixed oxide systems. However, it was hoped that this minimally funded effort would merely represent 'bridging-finance' to facilitate continuation of the research effort at a low level while hopefully awaiting a favourable AFOSR response to an unsolicited proposal aimed at allowing R&D on both points at a substantial level of effort; (Title of Proposal: *Extrinsic Surface States and Defects on Polycrystalline Solids: Characterization and Relevance to Electron Emission).* In the absence of a favourable response to that proposal for a substantial R&D effort on both points, results obtained on this minimally funded effort are necessarily incomplete. Nevertheless, the Principal Investigator expresses appreciation to EOARD for supporting this effort and believes that this support has made possible new results indicating the validity of surface reconstruction for mixed oxides and the important modifications thereby caused in surface properties.

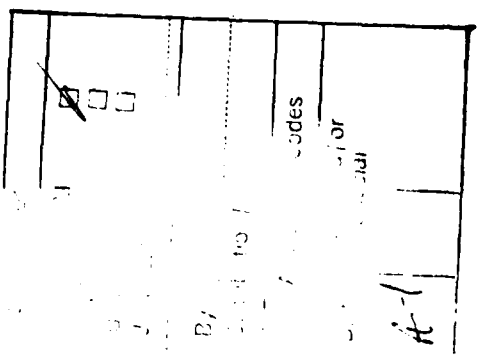

TABLE OF CONTENTS

INTRODUCTION

A new and relatively unexplored route to major modifications of the physical, chemical and catalytic properties of oxide-cathode-type solids is coming into focus as a result of recent work by the research group of the Principal Investigator of this Grant. Insights underlying this new route and its applications include:

(1) recognition that segregation of dopant to the surface layer of a solid can result from the strain energy associated with attempted incorporation of small amounts of a rather large dopant ion onto a sub-lattice comprising much smaller ions of similar valence. (A good example is Ba^{II} onto the cation sublattice of $Mg^{II}O$).

(2) Recognition that reconstruction/"rumpling" can occur in the surface layers of a solid to which a large dopant ion does segregate, thereby providing a surface-specific means for relaxation of strain energy.

(3) Recognition that relaxation of surface layers by such rumpling can not only produce surfaces distinguished by low surface energy (recall an analogy with the effect of a surface excess of a "surface-active" agent in lowering drastically the surface tension at Air-Liquid interfaces), but can also yield structures of reconstructed surfaces which intrinsically contain very large surface densities of dopant ions having high degrees of coordinative unsaturation.

(4) Recognition that the low surface energy of reconstructed

surfaces should result in materials with diminished tendency to sinter relative to the pure host material.

(5) Recognition that a large surface density of dopant ions enjoying high degrees of coordinative unsaturation within reconstructed surface layers may drastically alter the catalytic properties of the host material (recall the large modifications of the catalytic properties of platinum single-crystal surfaces introduced by relatively small surface densities of Pt_{cus} at step or kink sites).

A paper demonstrating partial realization of the potential of the foregoing ideas for modification of surface properties - in the specific case of the doping of MgO surfaces by Ba^{2+} - has already been presented, and is included as Appendix I of this report. In it are summarised the results of detailed computations (made by Wm. Mackrodt and co-workers) showing that segregation of Ba^{2+} to the surface of MgO was a strongly favoured process and revealing the very large reconstruction ("rumpling") of the Ba^{2+}/MgO surface computed to occur. Experimental studies showed furthermore that the incorporation of Ba^{2+} onto the MgO surface in monolayer - equivalent (m.e.) amounts drastically altered the surface photoluminescence, to the extent indeed that Ba^{2+}-related features totally dominated the surface photoluminescence in a manner consistent with the computed high surface density of Ba^{2+}_{cus} on the reconstructed surface. Experimental comparisons of the activity of Ba^{2+} doped surfaces for the decomposition of nitrous oxide (as a model test reaction) showed the expected dependence upon surface concentration of Ba^{2+}_{cus} on the

MgO. Experimental aspects of the new applications of these insights which have been attempted in this work will conveniently be sub-divided, in the following Technical Summary, into:

Type A Experiments

Preparative procedures aimed at producing alkaline earth oxides as small particles of high surface area, and then at doping surfaces of these materials with the large cation Ba^{2+} at monolayer (or submonolayer) equivalent amounts. The objective of the latter procedure was to achieve extensive reconstruction of surface layers. Also included under this heading are Results from preliminary efforts to characterise these and other conventionally prepared materials by spectroscopic and other physical methods.

Type B Experiments

Kinetic studies - utilising appropriate gas molecules as molecular probes - to test whether the reactivity/ catalytic activity of the monolayer-doped, mixed-oxides prepared by Type A studies is consistent with extensive reconstruction of the sample surface.

TECHNICAL SUMMARY

Results and Conclusions

Type A Experiments: Thermal decomposition of the corresponding carbonate, e.g. $SrCO_3 \longrightarrow SrO + CO_2$, is one conventional method by which alkaline earth oxides are produced as polycrystalline materials of high surface area during the preparation of 'oxide coated cathodes' for thermionic emission devices. Studies of this preparative route, and of the properties of SrO obtained in this way, have already been published elsewhere, and are given in detail as Appendix II to this report. However, the present study also included attempts to prepare barium oxide and magnesium oxide as very small particles of high surface area by an innovative and unconventional procedure which merits full description here. The equipment utilised for these innovative preparative attempts upon BaO and MgO was located in the research group of Professor H. Gleiter, Fachbereich 12.1, Werkstoffwissenschaften, Universitat Des Saarlandes, Saarbrucken, W. Germany. That research group has utilised the equipment with considerable success for the preparation of nanometer-sized particles of metals, particularly iron.[2] It is of relevance to note that the main interests of that group have been in the unusual physical (e.g. specific heat) and mechanical (e.g. very large densities of grain boundaries) of the metallic polycrystalline aggregates obtained upon compacting the very small particles of iron or gold obtained by routine operation of the equipment in the following manner :

Step 1: A conventional granular sample of the pure material is loaded onto a resistively-heated evaporation source (Tungsten or tantalum) which is then surrounded with a large metal bell-jar unit and evacuated to

ca. 10^{-7} torr with a turbo-molecular pump. Outgassing of the material is then conducted at temperatures just below that required for evaporation and the sample is cooled to RT in vacuo.

Step 2: After isolating the bell-jar unit from the pumps high purity helium is introduced at a static pressure in the range 1-10 torr. The purpose of the helium is to drastically shorten the mean-free-path of atoms evaporated (see below), and thereby to create conditions favouring collisons between the atoms and their aggregation into polyatomic particles before condensation onto a cold surface in the system.

Step 3: A cold surface with temperatures close to 77 K is created by cooling with liquid nitrogen a highly polished stainless-steel, cold-finger component of the bell-jar unit. By appropriate positioning of this cold-finger relative to the evaporation source, a convection current between evaporator and cold finger is created in the helium gas during heating of the evaporator.

Step 4: The evaporator temperature is raised slowly until evaporation just begins and manifests itself by the appearance of a thin black condensed layer upon that side of the cold finger which faces the evaporator. Condensation upon the surface at 77 K discourages any further aggregation of the particles other than that which occurred by collisons between the atoms

while being carried from the evaporator to the cold finger by the helium convection current. When a sufficient thickness of condensed layer is reached, the evaporator is cooled and the system is pumped out.

Step 5: The condensed layer (still at 77 K) is scraped off the cold finger in vacuo by a remotely-actuated ring-scraper fitted around the top of the cold finger for this purpose.

Our experiments with the above equipment were designed (i) to condense at 77 K deposits of BaO or MgO or BaO/MgO in which the oxides existed as very small particles (10-100 ion pairs); (ii) to scrape off these small-particle deposits at 77 K in vacuo into a quartz container and (iii) to measure luminescence spectra of the materials in vacuo for comparison with luminescence parameters we obtained (see data in Appendices I and II, on high surface area material prepared by conventional means.

Various modifications of the routine steps 2 and 5 above were attempted by the Principal Investigator during a one-month working visit at the laboratories of Professor Gleiter. The first and most obvious of these was to evaporate the metals, barium or magnesium in the normal way, but to introduce not only helium at moderate pressure (P_{He} of 4 to 10 torr were introduced in various experiments), but also oxygen at lower pressure (P_{O_2} of 1 to 10^{-3} torr were introduced) into the bell-jar. This modification had the objective of allowing Ba^{o} or Mg^{o} atoms to undergo oxidation to BaO or MgO molecules by collison with gas phase oxygen while being carried from evaporator to cold-finger on the convective currents of oxygenated helium. Experiments based on this modification were unsuccessful

for obtaining deposits of oxides. Instead, black condensed layers of metallic barium were obtained when barium was used in the evaporator and P_{O_2} was 1 torr. This lack of success can be attributed to the strong 'oxygen-gettering' properties of barium or magnesium metals which resulted in the initial static pressure of P_{O_2} being rapidly gettered by the granular metal when the latter was being heated in the evaporator. Subsequent evaporation then took place as Ba^{o} and there was insufficient oxygen left in the gas phase for oxidation to BaO to occur in the gas phase. Thus it became clear from experiments made using this modification that one or both of the following equipment modifications would be essential for this approach to have any chance of success in the future:

(i) Isolation of the Evaporation Source in its own Differentially Pumped/ Pressurised Chamber from which Oxygen can preferably be excluded;

(ii) Continuous Metered Introduction of Oxygen or possibly N_2O (see below) into the bell-jar to maintain a fixed, accurately-controlled value of P_{O_2} during formation of oxide ion-pairs and condensation of the oxide deposit.

Taking into account the lack of success with the modification just described, and also literature reports of the facile oxidation with oxygen of deposits of barium metal of thicknesses up to 100, nm even at temperatures close to ambient[3], another set of experiments was performed, based on the strategy of accepting that only evaporation and condensation of the metal as small particles was practicable with the equipment in its existing configuration (i.e. steps 1 to 4 carried out as described above). However, after step 4 efforts were made to oxidise the condensed metal deposit by introducing oxygen into the bell-jar, initially as a low dynamic pressure (ca. 10^{-2} torr) while the black deposit of metallic barium was maintained at 77 K. Although this visibly gave rise to a white exterior layer on the condensed deposit, underlying parts of the deposit visibly remained black thus

indicating only limited surface oxidation of the deposit. Visually it appeared that efforts to secure complete oxidation by the introduction of static oxygen pressures of up to 1 torr were unsuccessful. Indeed when Step 5 was attempted at 77 K with the partially-oxidised barium deposit in vacuo, a pyrophoric reaction was seen to begin at the top of the deposit and rapidly traverse its full length. It seemed probable that the exothermic process responsible for this was a reaction of an overlayer of barium peroxide with the underlying non-oxidised barium condensate, viz.

$$Ba^{o} + BaO_2 \longrightarrow 2BaO + Heat$$

Irrespective of the exact nature of the exothermic process, the traversal of the deposit by its high temperature reaction-front appeared highly detrimental to the chances of preserving any small-particle nature of the material scraped off the cold-finger. Examination of such material in an optical microscope did indeed indicate fusion into a film with large sub-units. An experiment in which the surface luminescence was tested with an experimental arrangement which had been shown to give good luminescence spectra with conventionally prepared oxide of high-surface area likewise indicated the fused material to be of very low effective surface area. Avoidance of incompletely oxidised layers in which barium peroxide and barium metal can be formed thus emerged as an essential aspect of any future attempts to obtain (and preserve) very-small-particle-type BaO. Progress towards this goal would seem more likely using: (iii) *N_2O rather than O_2 as oxidant since peroxide formation may then be less favourable than monoxide formation;* and/or (iv) *a technique, such as electron-beam or laser beam sputtering from BaO, in conditions such that BaO molecules (ion pairs) are favoured rather than metal atoms during evaporation.* Thus while these attempts at innovative preparative procedures for BaO and MgO yielded negative results with the equipment available at Saarbruken, valuable pointers were obtained towards the direction to be taken for future attempts.

Alternative and more conventional preparative procedure, fortunately, were employed in parallel with the innovative, but unsuccessful procedures just described. For each of the monolayer-doped materials desired for study, the same preparative strategy was adopted viz: Step a involved the preparation of the undoped single alkaline-earth oxide as a high surface area powder from the purest materials available (usually spectroscopically pure carbonate or oxide); Step b: consisted of treatments designed to purify the surfaces of these pure alkaline earth oxides,of residual carbon, without excessive annealing and loss of surface area, by calcinating them in oxygen at moderate temperatures, ca. 450°C. Parts of the materials thus prepared were utilised as extensively-dehydroxylated, 'pure reference oxide' powders against which to compare surface properties of monolayer-doped materials derived from them; Step c: involved controlled adsorption or ion-exchange procedures, aimed at achieving known monolayer or submonolayer coverage of the surfaces of one of the 'pure' reference oxides by a soluble ionic salt of barium or calcium. These procedures were carried out with alcohol, rather than with aqueous, solutions in order to avoid extensive rehydroxylation of the 'pure reference oxide' used as the support; Step d: Following vacuum-drying of the surface-doped material obtained in Step c, controlled heating in vacuo (monitored by mass spectrometry and by differential thermal analysis) was utilised to allow surface characterization of the adsorbed monolayer of ionic barium of calcium salt, en route to a surface layer of BaO or CaO. The resultant oxide-monolayer-doped material was then given additional heat treatments in vacuo to afford opportunities for surface reconstruction, whereby the monolayer of dopant oxide and the topmost layers of the host oxide could relax to give a 'rumpled' surface.

Utilization of steps (a)-(d), with MgO as the oxide support onto which a known amount of $Ba(NO_2)_2$ was incorporated at submonolayer-equivalent level via Step c, resulted in a Ba^{2+}/MgO material which yielded scanning electron microscope (SEM) pictures largely consistent with the declared objective of laying down BaO as a partial monolayer upon MgO particles *without* significantly altering the bulk properties of the MgO support. Some insights into the chemical changes occurring at the surface of the $Ba(NO_2)_2$-doped MgO material during step d are provided by part (a) of Figure A.1 below which summarises results of mass spectrometric monitoring of the release of nitric oxide, oxygen and water vapour during thermal outgassing. Detection and stoichiometry of nitric oxide and oxygen as major decomposition products are consistent with the stoichiometry

$$Ba(NO_2) \longrightarrow BaO + 2NO + \tfrac{1}{2}O_2$$

However, the considerable differences evident in figure Ala between the temperature regimes for release of nitric oxide (commencing at 700 K and extending to 1050 K) and release of molecular oxygen (875 K to 1050K) make it clear that oxygen product from the decomposition is retained much more strongly that the nitric oxide product . Use will be made below of the observations in accounting for rates of oxygen isotope exchange processes measured after outgassing of the $Ba(NO_2)_2$/MgO material to various temperatures

Plot A1(a): $Ba(NO_2)_2$ DECOMPOSITION PROFILE

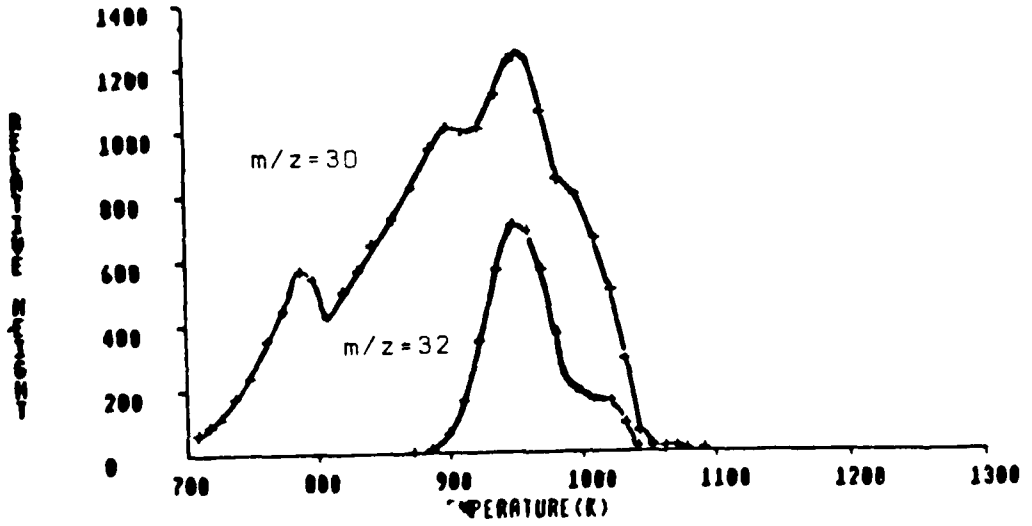

Differential thermo-gravimetric analysis (DTGA) of the SrO material and of the Ba^{2+}/SrO material - following unavoidable exposure to atmosphere subsequent to their preparation in vacuo - showed evidence for reformation of surface hydroxides and carbonates. However, the DTGA peaks corresponding to removal of these surface impurities were displaced by ca. 50°C to higher temperature for the Ba^{2+}/SrO material relative to SrO - as would be consistent with stronger binding of OH^-, HCO_3^- and CO_3^{2-} surface impurities upon the Ba^{2+}-doped surfaces. Similar effects have been observed in comparisons of DTGA of Ba^{2+}/MgO and MgO prepared via steps (a)-(d).

Spectroscopic measurements in the UV-visible upon the Ba^{2+}/MgO and Ba^{2+}/SrO materials prepared by steps (a)-(d) have not been completed at the time of writing this report. Such measurements have, however, been made, both as absorption (via diffuse-reflectance measurements) and as luminescence (via excitation and emission spectra) for samples prepared by an alternative conventional procedure, namely, the impregnation of soluble barium salts onto the surfaces of $SrCO_3$, $CaCO_3$ or $Mg(OH)_2$, followed by their activation in vacuo at 1273 K. Such materials yielded intense new photoluminescence features whose intensities varied in proportion to the level of doping of the surfaces by Ba^{2+}. *(cf. Figure I-1 of Appendix I)*. It could be concluded, on the basis of strong sensitivity of these Ba^{2+}-related luminescence features to quenching by small pressures of O_2 or N_2O, *(cf. Figure I-4 of Appendix I)* that the sites from which this luminescence originated were predominantly located at the surfaces of these Ba^{2+}/MgO, Ba^{2+}/CaO and Ba^{2+}/SrO samples.

The differential photoexcitation spectra shown in Figure (A2.) illustrate the extent to which the Ba^{2+}-related surface luminescence from these materials could be separated (on the basis of differing λ_{max} and/or differing spectral distribution) from luminescence of the corresponding undoped oxide. Excellent separability is clearly achieved for Ba^{2+}/MgO. That for Ba^{2+}/CaO might also form the basis of a spectroscopic method for evaluating the *surface* concentration of Ba^{2+}. However, the Ba^{2+}/SrO system, which approaches

most closely to the likely situation at the surface of oxide cathodes (particularly when non-operational after long periods of prior use), clearly would pose much greater problems for reliable assessment of surface Ba^{2+} concentration, $[Ba^{2+}]_s$, on the basis of differential photoexcitation spectroscopy (d.px.s.) utilising only differences in spectral distribution.

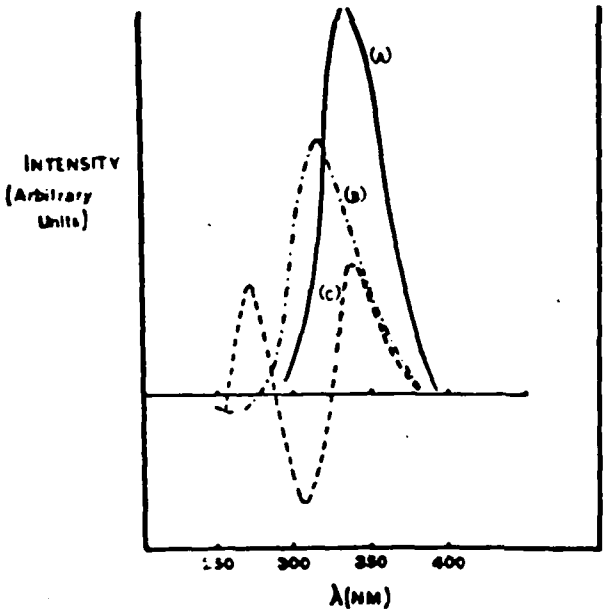

FIGURE A2a : Difference Excitation Spectra for BaO/MgO, Plot (A), BaO/CaO, Plot (B) and BaO/SrO, Plot (C). All samples at loading >3 m.e.

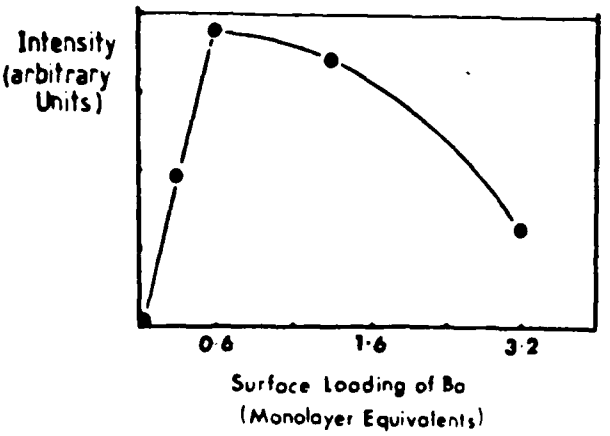

FIGURE A2b: Variation of Relative Intensities of Ba^{2+}-related Emission with $\lambda_{(max)}$ = 460 nm from Ba^{2+}/MgO samples having the Indicated Nominal Surface Loadings (monolayer equivalents) of Ba^{2+} (λ_{ex} = 335 nm).

Data in Fig.A2b show that at large differences in luminescence *intensity* between pure and Ba^{2+}-doped MgO surfaces could represent another basis for determining $[Ba^{2+}]_s$ $^{2+}$/MgO by d.px.s., at least up to ca. 0.6 monolayer equivalents of Ba^{2+}.

TYPE B STUDIES *(relating to interactions of 'probe' gas molecules, - including N_2O and ^{18}O-enriched oxygen gas - with thermally preactivated surfaces of polycrystalline alkaline-earth oxides. Appendices I and II should be consulted for full details of these experiments).*

Reference has already been made *(cf. Fig. I-4b in Appendix I)* to the strong quenching effect which low pressures of O_2 and N_2O exerted upon photoluminescence at room temperature from surface regions of Ba^+/MgO samples which had previously been thermally activated in vacuo at 1273 K.

Quenching by O_2 was fully reversible and disappeared when the O_2 was evacuated at 300 K, whereas only ~70% of the quenching effect of N_2O was removed by such evacuation. Decomposition of N_2O to give N_2 (but no O_2) product in the gas phase was shown by mass spectrometry to occur at pre-activated Ba^{2+}/MgO - N_2O interfaces in the same condition which gave irreversible quenching of photoluminescence *(cf. Fig. I-5 of Appendix I)*. It was concluded that quenching involved the destruction of luminescence centres by reaction at 300 K with the oxygen fragment from N_2O decomposition. Conversely, the totally reversible nature of the quenching by molecular oxygen pointed to only non-dissociative interaction of O_2 at 300 K with the luminescence centres upon preactivated Ba^{2+}/MgO surfaces.

Evidence for an important role of surface defects in the conversions of molecular-probe molecules upon the surfaces came from studies of the dissociation of N_2O over SrO (ex $SrCO_3$) surfaces at 758 K. Using both continuous-flow and pulsed-reactant techniques involving gas chromatography with thermal conductivity detection, clear evidence for defect-aided incorporation of oxygen fragments (from $N_2O \rightarrow N_2 + O$) into the oxide lattice emerged from strong upward deviation in the ratio of N_2 to O_2 product, but only in the pulsed reactant mode *(cf. Figure II-7 of Appendix II)*.

Steady-state rates of decomposition observed in the continuous-flow mode after large exposures to N_2O were not sensitive to, nor suitable for, detecting effects of surface defects - witness the fact that the ratio of N_2 to O_2 product took values of 2.0 ± 0.1 in such experiments.

Another gas-phase conversion which proved to be valuable as a molecular probe for active surface sites 'frozen-in' upon alkaline earth oxide surfaces following preactivation at high temperatures was the R_o-type oxygen isotope equilibration (OIE) process,

$$^{16}O_{2(g)} + {}^{18}O_{2(g)} \rightleftharpoons {}^{16}O{}^{18}O_{(g)} \quad \ldots\ldots R_o\text{-type OIE}$$

Following preactivation in vacuo at sufficiently high temperatures (> 1023 K), and rapid cool-down of the sample in a vacuum system free of H_2O or CO_2 vapours, SrO (ex $SrCO_3$) surfaces exhibited varying degrees of activity for this process when an equimolar mixture of $^{16}O_2$ and $^{18}O_2$ was introduced at room temperature. An approximately linear dependence of the extent of room temperature activity upon temperatures of preactivation above 1023 K *(cf. plot ii of Figure II-6a)* found for SrO surfaces which had not undergone a calcination step. This linear dependence was an important difference from temperature profiles claimed in the literature for development of photoluminescence features. The differences could be consistent: *either*, with less crucial importance of degree of coordination of ions at the surface for reactions of molecular probes thereon than for photoluminescence from the same surface; *or* alternatively with insensitivity of the rate-determining-step for the surface-assisted reaction towards the degree of coordination of surface oxide ions.

Samples of the 'pure reference oxides', MgO and SrO, - prepared in accordance with Steps (a) and (b) on page 9, which featured extensive sample reoxidation in a flow of oxygen at 450°C - only yielded activity

for the R_o-type OIE process at room temperature when they had been pre-activated in vacuo at temperature > 600° or 700°C respectively. Samples of Ba^{2+}/MgO prepared via steps (a)-(d) on page 9 likewise required pre-activation in vacuo at temperatures similar to that of the host MgO before R_o-type OIE would occur thereon at room temperature. Lower temperatures of preactivation did, however, bring about another oxygen isotope exchange process - namely the R_1-type OIE process at 500°C involving exchange of oxygen existing as surface oxide ions of the alkaline earth oxide materials with oxygen from the gas phase in accordance with,

$$^{16}O^{=}_{(\ell)} + {}^{18}O{}^{16}O_{(g)} \longrightarrow {}^{18}O^{=}_{(\ell)} + {}^{16}O{}^{16}O_{(g)} \quad \ldots R_1\text{-type OIE},$$

or

$$^{16}O^{=}_{(\ell)} + {}^{18}O{}^{18}O_{(g)} \longrightarrow {}^{18}O^{=}_{(\ell)} + {}^{16}O{}^{18}O_{(g)} \quad \ldots R_1\text{-type OIE}.$$

The dependence upon temperature of prior outgassing found for the R_o-type OIE at room temperature, as well as that found for the R_1-type OIE at a reaction temperature of 500°C, is illustrated in figure B1 on the following page. Plot B1b shows how τ_3^1, the time required for the initially (50% $^{16}O_2$ + 50% $^{18}O_2$) gas mixture to move 33% towards the final equilibrium composition of (25% $^{16}O_2$ + 25% $^{18}O_2$ + 50% $^{16}O^{18}O$), depended upon temperature of prior outgassing for the 'pure reference MgO' (plot 1) and for two samples of this material onto which submonolayer amounts of $Ba(NO_2)_2$ had been deposited. Comparison of this temperature dependence with that for the release of NO and O_2 - reproduced for convenience, and on the same temperature scale, in plot a - demonstrates that the R_o-type OIE did not become possible until <u>both</u> the NO and O_2 were removed from the surface. On the other hand, the dependence upon temperature of prior outgassing exhibited by the rate of the R_1-type OIE process (see plot c of Fig. B.1) makes it clear that active surface sites became available whenever the nitric oxide was released and when the oxygen fragment from decomposition of $Ba(NO_2)_2$ remained on the surface.

Plot (a): $Ba(NO_2)_2$ DECOMPOSITION PROFILE

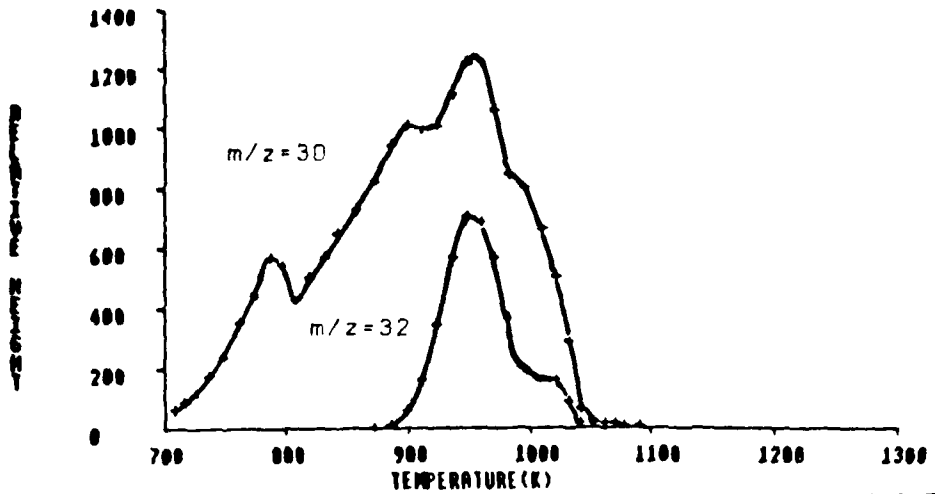

Plot (b): TIME TO 33% REACTION VS. ACTIVATION TEMPERATURE FOR THE R_0 TYPE OXYGEN ISOTOPE EXCHANGE REACTION AT ROOM TEMPERATURE.

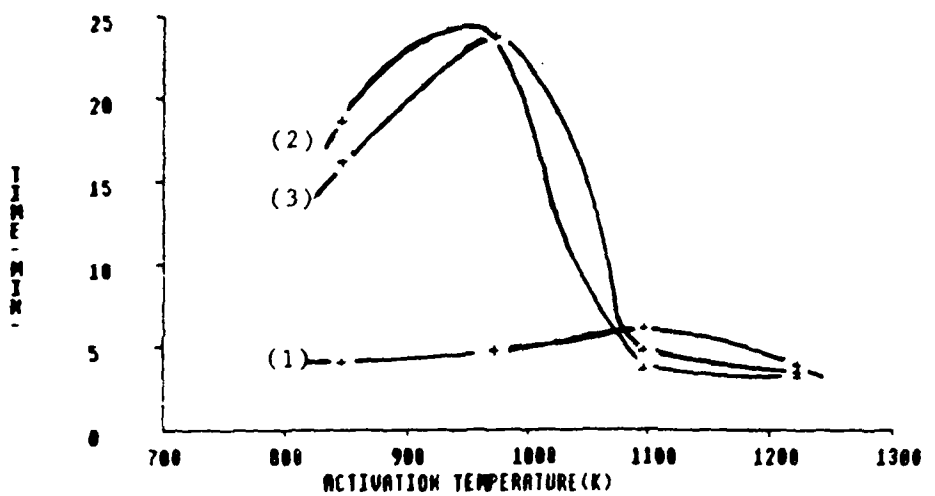

Plot (c): SLOPE(M.F. 34/36 VS. M.F.36 -0.5) VS. ACTIVATION TEMPERATURE FOR THE R_1 TYPE OXYGEN ISOTOPE EXCHANGE PEACTION AT 773 R.

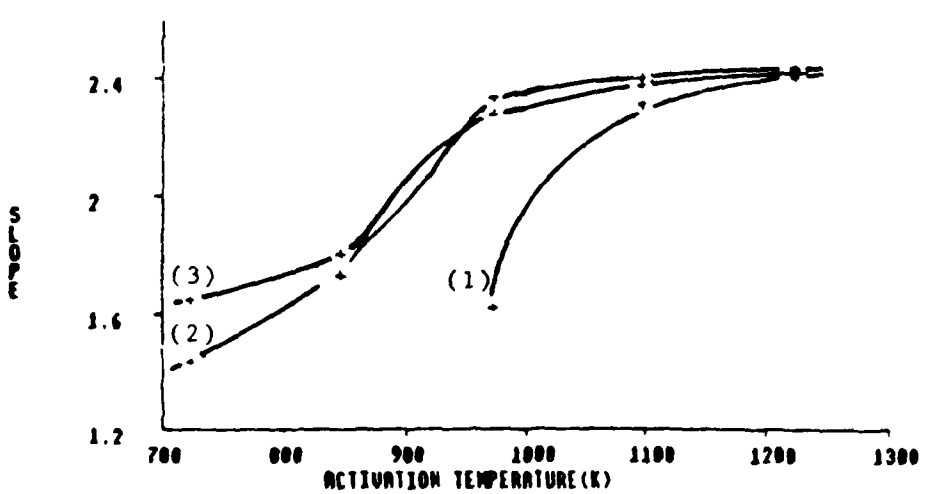

FIG. B-1: (a) THERMAL DECOMPOSITION OF $Ba(NO_2)_2$ AS STUDIED BY MASS SPECTROMETRY

(b) Ro TYPE EXCHANGE ON (1) MgO (2) $[Ba(NO_2)_2]_{low}$/MgO (3) $[Ba(NO_2)_2]_{high}$/MgO.

(c) R_1 TYPE EXCH ON (1) MgO (2) $[Ba(NO_2)_2]_{low}$/MgO (3) [Ba(N /MgO.

APPENDIX I

Spectroscopic and Kinetic Studies of Surface Processes on Alkaline Earth Oxides. Part 1: Effects of Ba^{2+} Dopant upon MgO

Paper Presented June 1984

at

Brunel University
Uxbridge
Middlesex UB8 3PH
UK

on

"ADSORPTION AND CATALYSIS ON OXIDE SURFACES"

And published in a book with that title

as

Volume 21 of Studies in Surface Science and Catalysis

(M. Che and G.C. Bond, (Editors)

Elsevier, Amsterdam, 1985 (pages 83-96)

SPECTROSCOPIC AND KINETIC STUDIES OF SURFACE PROCESSES ON ALKALINE EARTH OXIDES. EFFECTS OF Ba^{2+} DOPANT UPON MgO

J. NUNAN[1], J. CUNNINGHAM[1], A.M. DEANE[3], E.A. COLBOURN[2] and W.C. MACKRODT[2]

[1] Department of Chemistry, University College, Cork, Ireland

[2] I.C.I., New Science Group, Runcorn, Cheshire, England

[3] A.E.R.E., Harwell, Abingdon, England

ABSTRACT

Computations of the structural consequences of segregation of Ba^{2+} at monolayer and submonolayer coverages on (001) surfaces of MgO indicate extensive reconstruction. The predicted reconstruction for Ba^{2+}/MgO contrasts sharply with insignificant reconstruction reported for pure MgO surfaces. Results are described for experimental comparisons of the surface luminescence and surface reactivity of high surface area samples of Ba^{2+}/MgO with MgO and BaO. Extent of agreement is assessed between the observed Ba^{2+}-related effects and these working hypotheses: (i) that the Ba^{2+} induces surface reconstruction of the type calculated, to yield surface anions and cations in positions of altered, but non-integral, co-ordination; (ii) that photoexcitation of electrons at such O^{2-}_{cus} sites are responsible for enhanced luminescence; and (iii) that Ba^{2+}_{cus} sites are involved in enhanced reactivity towards N_2O at 300 K.

INTRODUCTION

Luminescence and reactivity of surfaces of alkaline earth oxides are the particular facets of Tony Tench's distinguished and many-facetted contributions to the study of metal oxides which will primarily concern us in this paper. Thanks largely to the spectroscopic equipment and sample pretreatment procedures developed in Tony's laboratory (ref. 1-3), it became possible to attain and characterise reproducible spectroscopic parameters (cf. table 1) for the luminescence detectable from high surface area samples of alkaline earth oxides. The development of a conviction that extrinsic surface states were strongly implicated in this and other properties of high surface area ionic (h.s.a.i.) oxides soon became evident (ref. 4,5). Indeed, a confluence of such proposals by Tench and co-workers concerning surface luminescence with those from Stone and co-workers (ref. 6-9) concerning diffuse reflectance from h.s.a.i. oxides contributed to interpretation of these spectroscopic features in terms of surface-exciton (s.e.) models. As the name implies, such s.e. models recognise important differences between excitons at the surface (a correlated hole-electron pair produced at the surface by the absorption of an appropriate photon in the visible or near-uv) and those within the bulk. Equation 1 summarises one formalism adopted in the literature to allow distinction to be made between excitons on the basis of differences between the extent of co-ordination (or conversely the extent of co-ordinative unsaturation) of the ion sites involved. Subscripts nc in this

$$(O^{2-}_{nc}\ ,\ M^{2+}_{nc}) \underset{h\nu'(lum)}{\overset{h\nu(abs)}{\rightleftharpoons}} (O^{-}_{nc}\ ,\ M^{+}_{nc})^{*} \qquad \text{Eq. 1}$$

equation denotes the degree of co-ordinative saturation of the lattice oxygen anion from which (in the one-excited electron approximation) an electron is

excited upon absorption of a photon, or to which it returns in radiative decay of an exciton. Within the bulk, n = 6 at regular lattice sites, whereas n is reduced to 5 with concomitant decrease in Madelung potential for ions at planar non-defective regions of (100) surfaces of MgO or other alkaline earth oxides. Further reductions of n to 4 at surface defect locations (such as an edge or step upon the (100) surface), or to 3 at a defect site of high co-ordinative unsaturation (such as a corner or kink site), have also been envisaged. Satisfactory agreement has been reported by Stone (ref. 9) between transition energies calculated for hν(abs) of Eq. 1, on the basis of static Madelung potentials appropriate to n = 5, 4 & 3, and features (usually three in number) partially resolved in the diffuse reflectance spectra of MgO, CaO, SrO and BaO. It is worth noting the relatively large magnitude of the red-shifts, e.g. up to 3.5 eV in the case of MgO, which these calculations seek to account for in terms of differences in static Madelung potential envisaged for O_{nc}^{2-} having n = 6, 5, 4 or 3. Results of some recent experiments and computations have called into question the wisdom/validity of seeking thus to account for such large red-shifts mainly in terms of diminished static Madelung potential at surface defect locations whereon n takes the integral values of 3, 4 or 5. Computations have been made with models which simulate defective non-planar surface regions whereon some surface ions are initially positioned at corner/kink sites for which n would nominally be 3, and some at edge/step sites for which n = 4 (ref. 10). Such computations indicate that, in marked contrast to ions having n = 5 at flat non-defect terraces (ref. 10), ions at surface defect positions may experience large relaxation, e.g. up to 0.45 Å inward for O_{4c}^{2-} in its ground electronic state. The accuracy of earlier calculations which ignored such relaxation - as was implicit in their use of static Madelung potential and their restriction of n to the integers 3, 4 or 5 - may be questioned on this basis. Another incompletely resolved question

is the possibility that surface impurities/adsorbates located in the immediate proximity of surface O^{2-}_{nc} may influence the transition energy and/or probability for the optical transitions in eqn. 1, e.g., very recent reinvestigation of the luminescence from h.s.a.i. MgO points to the involvement of surface hydroxyls (ref. 11) in photoexcitation at 270 nm.

EXPERIMENTAL

Approach

The unresolved questions detailed in the introduction have here been addressed by a combination of: (a) computations aimed at predicting the effect of a surface impurity viz. Ba^{2+}, upon the structure of (001) faces of MgO and (b) experimental determination of the influence of Ba^{2+} surface dopant upon surface luminescence and surface reactivity of h.s.a.i. MgO. Details of the computational approach are given elsewhere in detail (ref. 12).

Materials

Steps for incorporation of Ba^{2+} dopant onto MgO consisted of adding 5 g of $Mg(OH)_2$ to aqueous $Ba(NO_3)_2$ containing the desired number of moles of Ba^{2+}, heating first to dryness and then at 600 K to convert $Mg(OH)_2$ to MgO and finally at 780 K to decompose $Ba(NO_3)_2$ to BaO. Evolution of gases at these various stages was monitored by mass spectrometry (Vacuum Generators Micromass 6), and also during subsequent activation of the material in vacuo while the temperature was increased stepwise from 780 to 1273 K. Two considerations made it highly unlikely that Ba^{2+} would migrate significantly into the lattice of the supporting oxide during such preparations: Firstly, the results of recent computations (ref. 12) showing that Ba^{2+} should have a strong tendency to segregate to the surface of MgO, CaO or SrO; and secondly, large energies, ca. 5 eV, for diffusion of cations via cation vacancy or interstitial mechanisms

TABLE 1

PARAMETERS OF OBSERVED SURFACE LUMINESCENCE FROM Ba^{2+}-DOPED MgO and RELEVANT PROPERTIES OF MgO and BaO

Nominal surface loading by Ba^{2+} /monolayer equiv.	Luminescence Parameters: Excitation λ max	Emission λ max	Surface Area /m^2 g^{-1}	$I(Ba^{2+}-/MgO)$ @ 460 nm / I(MgO) @ 394 nm **
3.2 m.e. Ba^{2+}/MgO	280(vs)*	→ 460(vs)	58	
	340(vs)	→ 460(vs)		~ 10
1.6 m.e. Ba^{2+}/MgO	280(s)	→ 456(s)		
	335(s)	→ 456(s)		~ 15
0.6 m.e. Ba^{2+}/MgO	280(s)	→ 452(vs)		
	330(s)	→ 452(vs)		~ 20
0.3 m.e. Ba^{2+}/MgO	278(s)	→ 416(m)		
	330(w)	→ 450(w)		~ 5
0.06 m.e. Ba^{2+}/MgO	270(s)	→ 394(s)		~ 1
undoped MgO	270(s)	→ 394(s)	92	1.0
undoped BaO	280(vw)	→ 460(vw)	4.9	~ 10^{-2}

* Notations (vs), (m), (vw), etc., denote whether the luminescence feature was very strong, moderate or very weak, etc.

** Heading of the last column refers to the intensity ratio of emission at indicated wavelengths.

(ref. 13). The loadings of the host oxides with Ba^{2+} achieved by these procedures are, therefore, better expressed as monolayer equivalents (m.e.) than as mole percent relative to the weight of the support. The surface areas used in estimating the coverage as m.e. are listed in Table 1 and were determined at the CSIC Institute of Catalysis Madrid (courtesy of Dr. J.G. Fierro).

These estimated values of m.e. should be regarded as upper limits since some evidence for small microcrystallites of BaO (i.e. existing as other than monolayer dispersions) was found by transmission electron microscopy (courtesy of Madame Leclerq, CNRS, Institute of Catalysis, Lyon) for a sample of Ba^{2+}/MgO with nominal loading of 3.2 m.e.

Spectroscopic Measurements

Preconditioning of the powdered samples in vacuo for 4 hours at 1273 K, whilst protected by liquid - N_2-cooled traps, was carried out in quartz sample holders prior to observations of their luminescence or diffuse reflectance spectra under front-surface illumination. Each holder had a rectangular section with parallel flat faces 2-3 mm apart into which the powders usually were shaken after preactivation and seal-off at the background pressure, ca. 10^{-6}, torr of the conventional vacuum system. When effects upon luminescence by the addition and/or removal of gases were to be determined, the sample of oxide was preactivated in situ within the rectangular section whilst remaining attached to a vacuum system at the spectrometer. The instrumentation used in obtaining the excitation/emission spectra has previously been described in detail (3). Excitation was provided by a 250 W Xenon lamp from which appropriate wavelengths were sequentially selected using two coupled Spex 14 monochromators whilst taking excitation spectra. A single Spex monochromator placed between sample and detector was held at a fixed wavelength and augmented by appropriate cut-off filters in taking excitation spectra. Spectra were automatically corrected for variations in excitation intensity with time or changing wavelength via instrumental comparisons (with an Ortec photon-counting system) of the pulse rates from two monochromators, one monitoring luminescence intensity and the other the intensity of the source at the same wavelength. Excitation spectra at acceptable signal.noise ratio were only obtained upward from 230 nm,

due to low source intensity at shorter wavelengths. Sharp cut-off filters (Corning 3-74 and O-52) were placed between the sample and the emission monochromator to minimise scattered wavelengths from the xenon source reaching the photomultiplier. A band-pass of 5 nm was used for both the excitation and emission results.

Measurement of Surface Reactivity

Largely on the basis of published evidence (ref. 14,15) that co-ordinatively unsaturated cations act as active sites for each process on other oxides, the gaseous conversions used to assess reactivity of the surface at 300 K after vacuum preactivation at selected temperatures were as follows:

$$N_2O(g) \rightleftharpoons N_2O(ads) \xrightarrow{ne^-} N_2(g) + O^{n-}(ads) \qquad 2a$$

and

$$^{16}O_2 + {}^{18}O_2 \rightleftharpoons 2\,{}^{16}O{}^{18}O(g) \qquad 2b$$

Progress of each conversion was monitored by mass spectrometric analysis of gas samples taken at intervals from a static reactor following admittance of pure nitrous oxide or (50% $^{16}O_2$ + 50% $^{18}O_2$) at 300 K.

RESULTS AND INTERPRETATION

Computations

Figure 1 summarises results of computations indicating large reconstruction ('rumpling') effects of (100) surfaces of MgO whenever high concentration of Ba^{2+} are heavily segregated to the surface (i.e. approaching monolayer coverage by Ba^{2+}). In relation to Ba^{2+}/MgO the following predictions should particularly be noted from this figure: (i) that all surface anions, O_s^{2-}, experience an outward displacement by 0.79 lattice units; (ii) that the

surface entity experiencing the greatest outward displacement - and hence the greatest degree of co-ordinative unsaturation - is that sub-set of surface cations, Ba^{2+}_{cus}, displaced by 1.21 lattice units; (iii) that the remaining 50% of surface Ba^{2+}_{s} experience a relatively small displacement by 0.38.

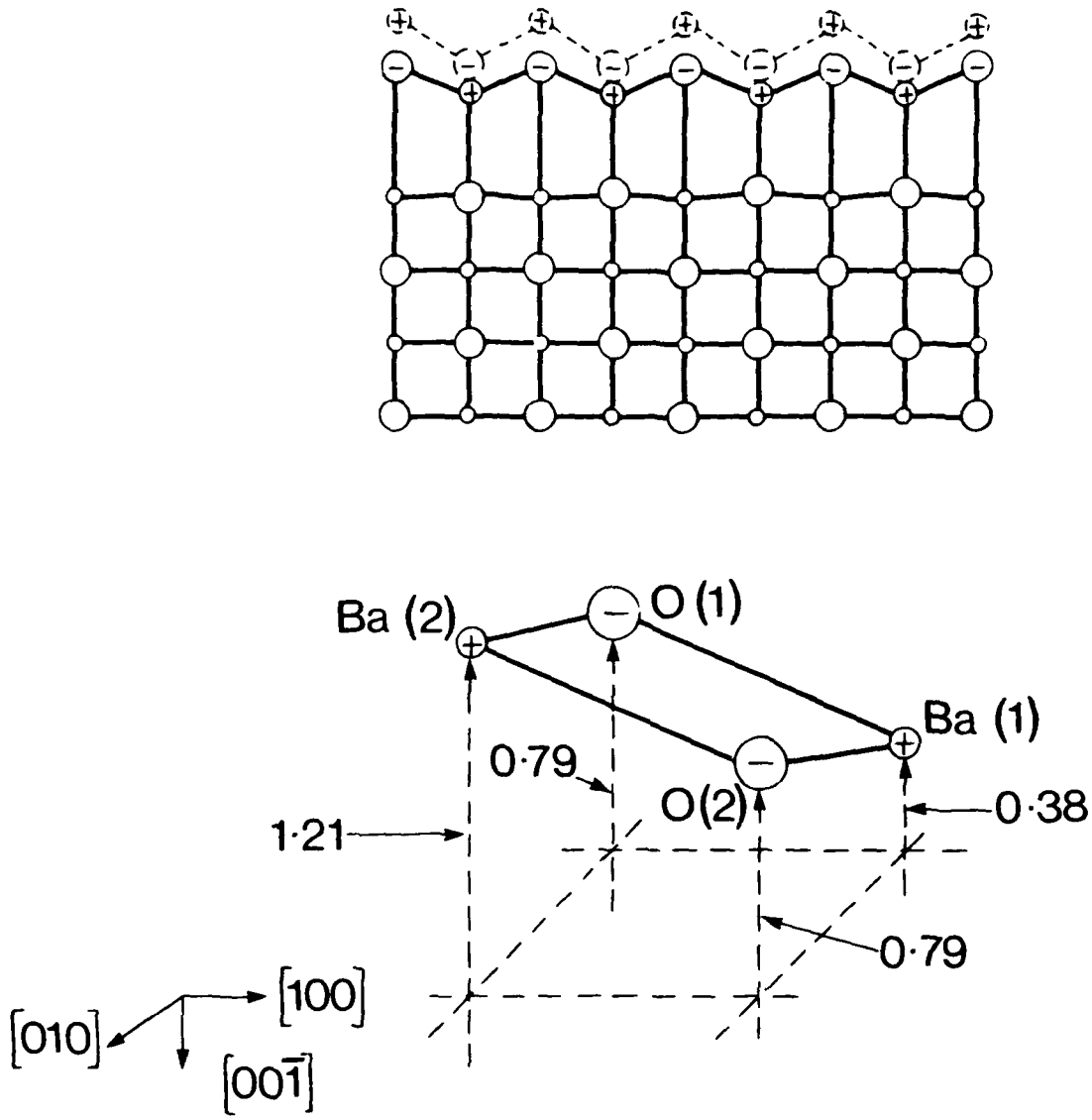

Fig.B1. Results of computations showing the reconstruction ('rumpling') of MgO surfaces having Ba^{2+} heavily segregated (to monolayer equivalent) to the surface. Numbers indicate (in lattice units) the outward displacement of two Ba^{2+} and two O^{2-} representing a unit cell of the reconstructed surface.

Spectroscopic Ba^{2+}/MgO

Figure 2 demonstrates the striking changes brought about in the luminescence from MgO following incorporation of Ba^{2+} onto its surface. The excitation spectra shown in Part A of the figure show that, whereas undoped MgO gave rise to a single excitation band with λ_{max} = 270 nm following preactivation of 1293 K in vacuo, (cf. plot A1), the Ba^{2+}.MgO sample with a barium loading nominally equivalent to 3 m.e., gave two bands in its excitation spectrum with peaks at λ_1 = 277 and λ_2 = 340 nm respectively. Figure 2B illustrates the influence of decreasing the Ba^{2+}-doping level upon excitation features for a series of Ba^{2+}/MgO samples : — a rapid drop in the excitation feature of the MgO support should particularly be noted. This shows that the relative intensity of this excitation feature reflects the level of doping by Ba^{2+}. A more complex situation, originating from overlap of the Ba^{2+} feature and those of the MgO support, clearly existed for the excitation feature with strong excitation intensities at 260-290 nm. The position of λ_{max} for this feature was close to the 270 nm position characteristic of the MgO support. Assignment of the Ba^{2+}-related excitation feature at 340 nm to luminescence as per eqn. 1, but involving surface O^{2-} displaced outward by 0.79 to positions of lower co-ordination, in the manner predicted by computations and summarised in Fig. 1, represented an attractive working hypothesis for explanation of the red-shift of λ_{max} for this excitation. Evidence will emerge in the following paragraph that this working hypothesis can also help to account for greatly enhanced luminescence intensity from Ba^{2+}/MgO relative to MgO or BaO. Plots of intensity of emitted luminescence versus wavelength of emission are compared for Ba^{2+}/MgO and MgO in Fig. 2C. It may be noted that whereas MgO under excitation at 270 nm gave emission λ_{max} at 395 n, (cf. plot (i) of Fig. 2C), excitation of heavily doped Ba^{2+}/MgO at either 280 or 340 nm (cf. plot(ii) of Fig. 2C). The results of preliminary studies of the dependence upon Ba^{2+}

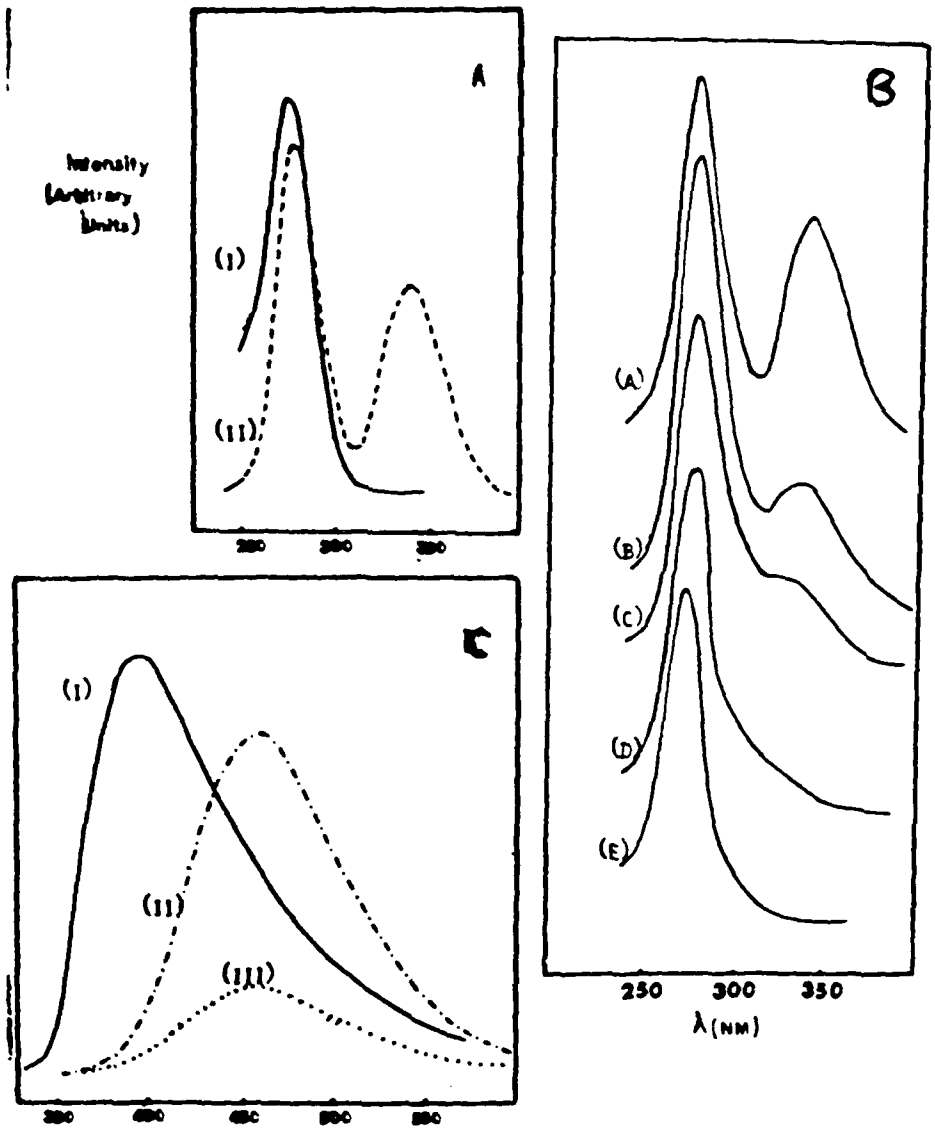

Figure B2. Effect of Ba^{2+} surface dopant upon photoexcitation, (Parts A and B), and luminescence/emission spectra, (Part C), relative to undoped MgO: 2A, Plot I, pure MgO, Plot II 3.2 m.e. Ba^{2+}/MgO; 2B Dependence of excitation features at 340 nm upon following nominal loading of MgO surface by Ba^{2+} - 3.2 m.e. (A), 1.6 m.e. (B), 0.6 m.e. (C), 0.3 m.e. (D) and 0.06 m.e. (E); 2C Differences in spectral distribution of emission from pure MgO (Plot I) and from 3.2 m.e. Ba^{2+}/MgO excited at 340 nm (Plot II) or 280 nm (Plot III).

dopant level exhibited by the intensity at 460 nm, I(460), and by $\lambda_{(max)}$ for the emission are summarised in Table 1. These demonstrate firstly that for Ba^{2+} loadings > 0.6 m.e., $\lambda_{(max)}$ for emission remained at 456 ± 5 nm whether excited at 280 or 335 ± 5 nm and that I (460) did not increase significantly with loading but rather declined slowly in this high-loading range. Secondly, the data for loadings < 0.6 m.e. show a precipitous drop in I (460) with diminishing loading and a parallel displacement of $\lambda_{(max)}$ away from 460 nm and back towards the $\lambda_{(max)}$ = 416 nm at 0.3 m.e. and $\lambda_{(max)}$ = 394 nm at 0.06 m.e. These results make it clear that only for loadings << monolayer did the emission of the support 'show through' clearly, whilst at moderate and high loadings the Ba^{2+}-related emission strongly predominated. In terms of the working hypothesis developed in an earlier paragraph this may be understood on the basis that, relative to a low surface density of defect-related O^{2-}_{nc} locations upon non-reconstructed MgO surfaces, the Ba^{2+}-induced rumpling of the Ba^{2+}/MgO surfaces caused a massive enhancement in the surface density of O^{2-}_{s} displaced into positions of diminished co-ordination (cf. Fig. 1A) and emitting at ca. 460 nm in analogous fashion to eqn. 1.

Preparation of h.s.a.i. BaO powder by thermal decomposition of $BaCO_3$ or $Ba(NO_3)_2$ was attempted with a view to comparing the luminescence parameters of the unsupported BaO with those just described for Ba^{2+}/MgO. Luminescence from the BaO preparations was, however, orders of magnitude less intense than from Ba^{2+}/MgO samples, making it necessary to employ a 410 nm cut-off filter to diminish scattered/incompletely-monochromatised photons from the excitation source to flux levels comparable to any very weak luminescence at > 410 nm from the BaO samples. Emission spectra obtained in these conditions are shown in Fig. 3A, where a broad emission centred around 450 nm can be seen as well-developed for BaO ex-$BaCO_3$ but less well so for BaO ex-$Ba(NO_3)_2$. Only this emission feature seemed characteristic of BaO, since the broad and comparably

weak emission centred around 550 nm in Fig. 3B was traced to the silica walls of the sample holder. Figure 3A shows excitation spectra obtained at rather poor signal-to-noise ratio by monitoring emission at 450 ± 10 nm from the BaO samples. Two excitation bands may be discerned having $\lambda_{(max)}$ at 275 ± 10 and 340 ± 10 nm. The latter coincides, within the appreciable experimental error, to $\lambda_{(max)}$ for the excitation feature which was very strong for Ba^{2+}/MgO samples (cf. Fig. 2A).

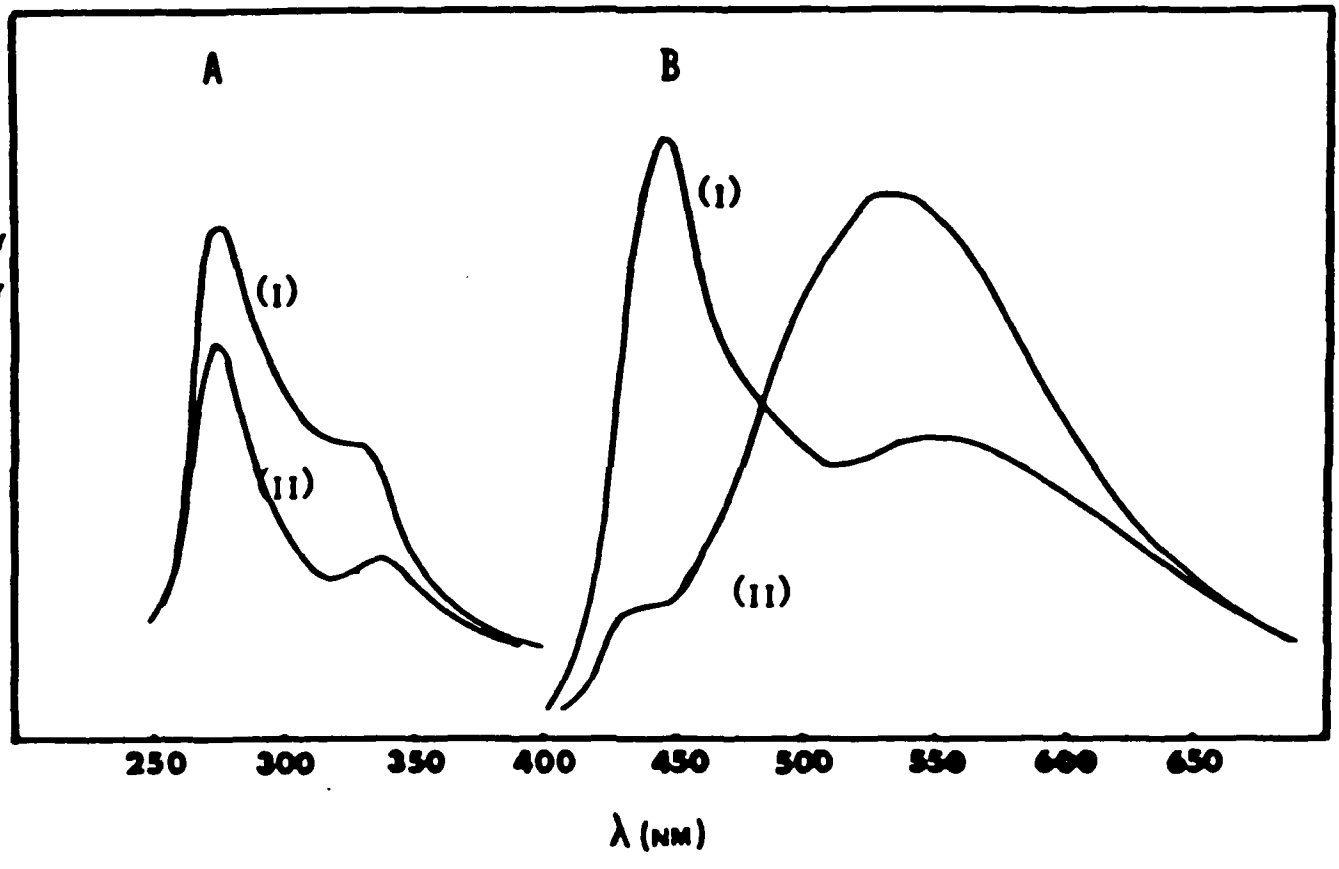

Figure B3. Excitation (Part A) and Emission (Part B) spectra at 293 K of unsupported BaO prepared from $BaCO_3$ and $Ba(NO_3)_2$; A(i) and (ii) respectively are excitation spectra of BaO prepared from $BaCO_3$ and $Ba(NO_3)_2$ monitored at emission wavelength = 460 nm); B(i) and (ii) are emission spectra of BaO, ex. $BaCO_3$ and $Ba(NO_3)_2$ respectively, excited at 335 nm.

Figure 3 thus lends support to the use of emission at 455 ± 10 nm and of excitation at 340 ± 10 nm - both features being of very low intensity - as spectroscopic indicators of electronic transitions occurring at environments similar to those provided by the surface of BaO. In the literature, the relatively low surface areas measured for BaO, and the assumed lower density of surface defects, have been given as reasons for the notably low intensity of such features (ref. 8). While present results are not in conflict with such interpretation, the great enhancements in intensity which we observe (at similar transition energies) from Ba^{2+}/MgO point towards operation of another factor additional to surface area-increase and factor-of-10 proportionate increase in defect-related O^{2-}_{nc}. As envisaged in our working hypothesis, reconstruction of the Ba^{2+}/MgO surfaces can be such an additional factor. This would not be inconsistent with the observed similarities in $\lambda_{(max)}$ for excitation and emission from BaO and Ba^{2+}/MgO, since on both surfaces Ba^{2+} would be the nearest cation neighbours to the O^{-}_{cus} sites involved in transitions (cf. Fig. 1).

Effects of Gases upon Luminescence at 300 K

Convincing evidence that the sites involved in luminescence from heavily doped Ba^{2+}/MgO (Ba^{2+} loading nominally 3.2 m.e.) were located predominantly at the surface came from observations upon the sensitivity of luminescence to (i) the gases H_2, CH_4, O_2 and N_2O, and (ii) the rigour with which residual gases were removed in the preparation and outgassing procedure. Thus the intensity of the Ba^{2+}-related excitation feature at 340 nm was five-fold greater than that at 277 nm for rigorously outgasses samples, unlike the rather similar integrated intensities of these two excitation features in samples given the routine outgassing pretreatment (cf. plot(i) of Fig. 4 with Fig. 2A). Daley very recently reported that prolonged outgassing of $Mg(OH)_2$ powder at 1200 K

diminished a photoexcitation feature attributed to intrinsic excitations of OH^- ion in the $Mg(OH)_2$ structure (ref. 11). Some final breakdown of surface $Mg(OH)_2$ may have likewise contributed to the diminution of the photoexcitation feature at 277 nm in our prolonged outgassing of Ba^{2+}/MgO at 1273 K. However, our observations that the introduction of H_2 at 300 K restored intensity to the photoexcitation feature at 277 nm and that this enhancement could be reversed by 2.5 h outgassing at 300 K (cf. Fig. 4) suggest an interesting alternative explanation, viz. that some H_2 released during breakdown of $Mg(OH)_2$ remained as residual gas within the sample cell when sealed off in the routine outgassing procedure, whereas such residual gas was removed during the more rigorous outgassing procedure. A reversible enhancement of the 277 nm photoexcitation feature of Ba^{2+}/MgO was also observed with introduction/removal of CH_4. Reversibility at 300 K implies a weak interaction between the luminescence sites and H_2 or CH_4, rather than a strong interaction such as dissociative chemisorption. Indeed our observation on the influence of H_2 and CH_4 on luminescence do not require any interaction with the ground state of the surface locations involved - only with their excited state.

Almost complete quenching of the Ba^{2+}-related luminescence features of Ba^{2+}/MgO resulted when either of the oxidising gases O_2 or N_2O was present (cf. Fig 4B) at pressures ca. 1 torr. Evacuation of the gas at 300 K reversed this quenching almost totally for $O_2/Ba^{2+}/MgO$, but only partially (ca. 60%) in the case of $N_2O/Ba^{2+}/MgO$. Following other workers, who observed a reversible quenching by O_2 at undoped MgO and CaO and attributed it to formation of a weak complex with the electronically excited surface locations (refs. 2,6), quenching may be understood as the result of competition between radiative decay of surface excitons (cf. eqn. 1) and their diversion, as follows, into non-radiative decay via exciplex formation with O_2 and N_2O as oxidising gases

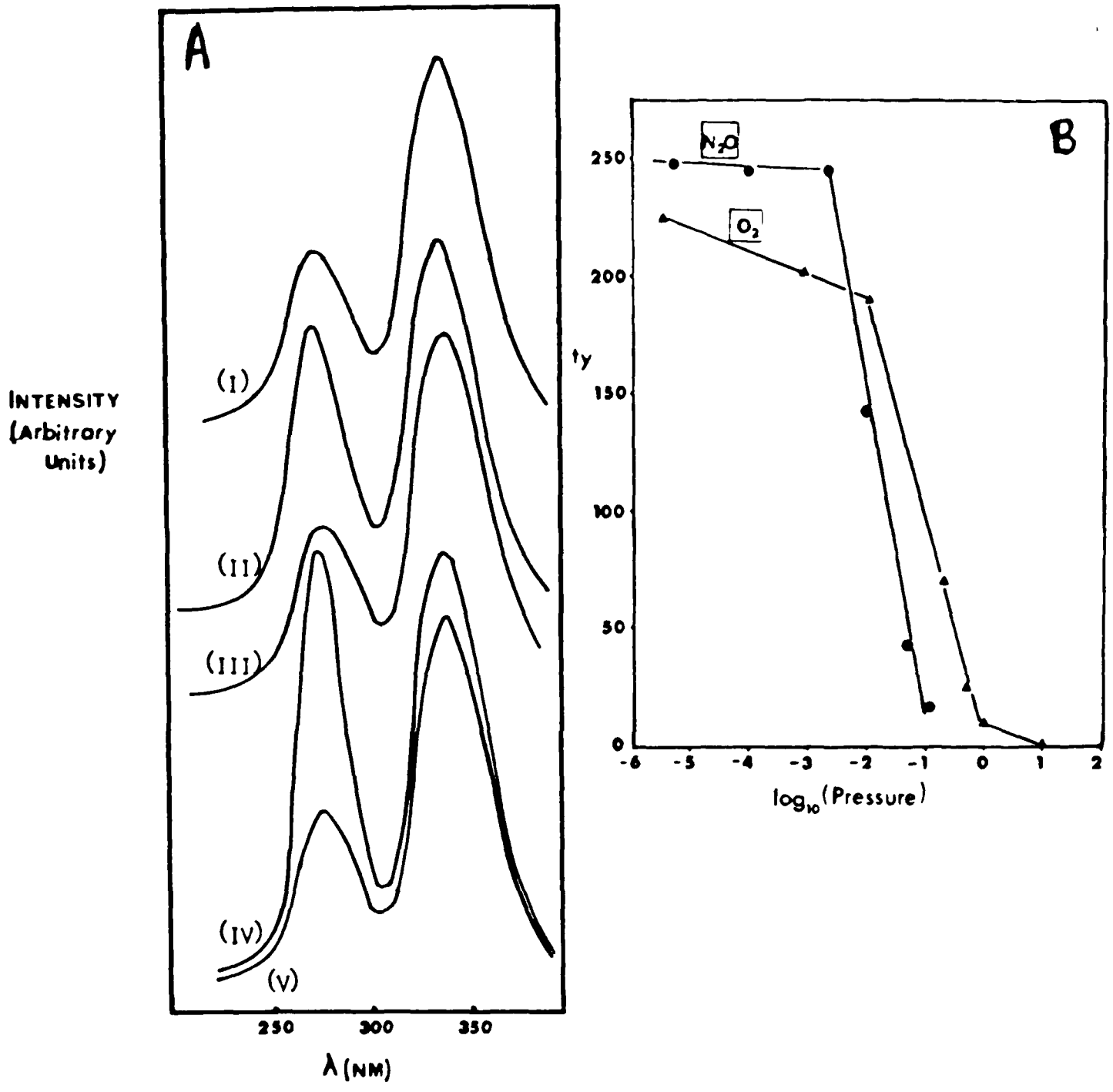

Figure B4. Effects of reducing gases (Part A) and oxidising gases (Part B) upon Ba^{2+}-related luminescence features of 3 m.e. Ba^{2+}/MgO: 4A photoexcitation spectra after: (I) enhanced outgassing; (II) contact with 10^{-2} torr H_2; (III) contact with 1 torr H_2; (IV) upon evac. of H_2; (V) after 3 h outgassing to 10^{-7} torr. 4B Extent of quenching of emission of 460 nm in the presence of indicated pressures of N_2O or O_2 at 300 K.

$$A(g) + (M^{+}_{cus} , O^{-}_{cus})^{*} \rightleftharpoons [A\text{----}^{*}\text{----}(M^{+}_{cus} , O^{-}_{cus})] \qquad \text{Eqn. 3a}$$

$$[A\text{----}^{*}\text{----}(M^{+}_{cus} , O^{-}_{cus})] \longrightarrow A(g) + (M^{2+}_{cus} , O^{2-}_{cus}) \qquad \text{Eqn. 3b}$$

Quenching via such a charge-transfer-type exciplex avoids the need for significant complex formation in the ground state (recall difficulties reported in the literature in forming significant surface concentration of O_2^- on alkaline earth oxides ref. 16). Relative rate-coefficients for such electron-donor-acceptor type quenching by electron acceptors having differing electron affinities (e.a.) commonly decrease with decreasing e.a. However, our experimental observations showed the opposite to be the case, viz. that for any pressure in the range 10^{-2} to 10^{-1} torr, N_2O (e.a. ~ 0.1 eV) produced stronger quenching than O_2 (e.a. ~ 0.5 eV) at the same pressure (cf. Fig. 4B). This anomaly suggested that eqn. 3a and 3b on their own were not an adequate description of processes at the $N_2O/Ba^{2+}/MgO$ interface at 300 K. Subsequent paragraphs provide evidence of other interactions.

Surface Reactivity Studies at 300 K

Figure 5 demonstrates that samples of Ba^{2+}/MgO preactivated in vacuo at temperatures 1093-1293 K, i.e. in similar manner and across similar temperature range to that required for development of luminescence, retained an ability, after cooling to 300 K, to decompose carefully pre-purified N_2O, but to a rather limited extent. Maximum extent of this limited decomposition, is seen in Fig. 5A to have arisen after preactivation at 1183 rather than at 1093 or 1273 K, and corresponded to development of a partial pressure ca. 2×10^{-4} torr of N_2 in the static reactor. Since no O_2 product was detected in the gas phase and more N_2O was lost from the gas phase than the amount of N_2 detected, the observations were fully consistent with eqn. 2a. On that basis it seems reasonable to attribute the observed irreversible component in luminescence

quenching by N_2O at 300 K to deactivation of some surface locations via irreversible N_2O dissociation thereon, as per the last step of eqn. 2a. It is important to recall from previous work that the availability of one or more excess electrons in the immediate vicinity has been recognised as a necessary, enabling feature of such decomposition sites (*ref. 14*). *In respect of the* observed reversible component of quenching by N_2O, present data do not suffice to determine whether this was mediated by $N_2O(ada)$, or $N_2O(g)$, or by both. Nor do they suffice to examine possible inter-relationships of P_{N_2O} with extent of decomposition and relative amounts of reversible and irreversible quenching.

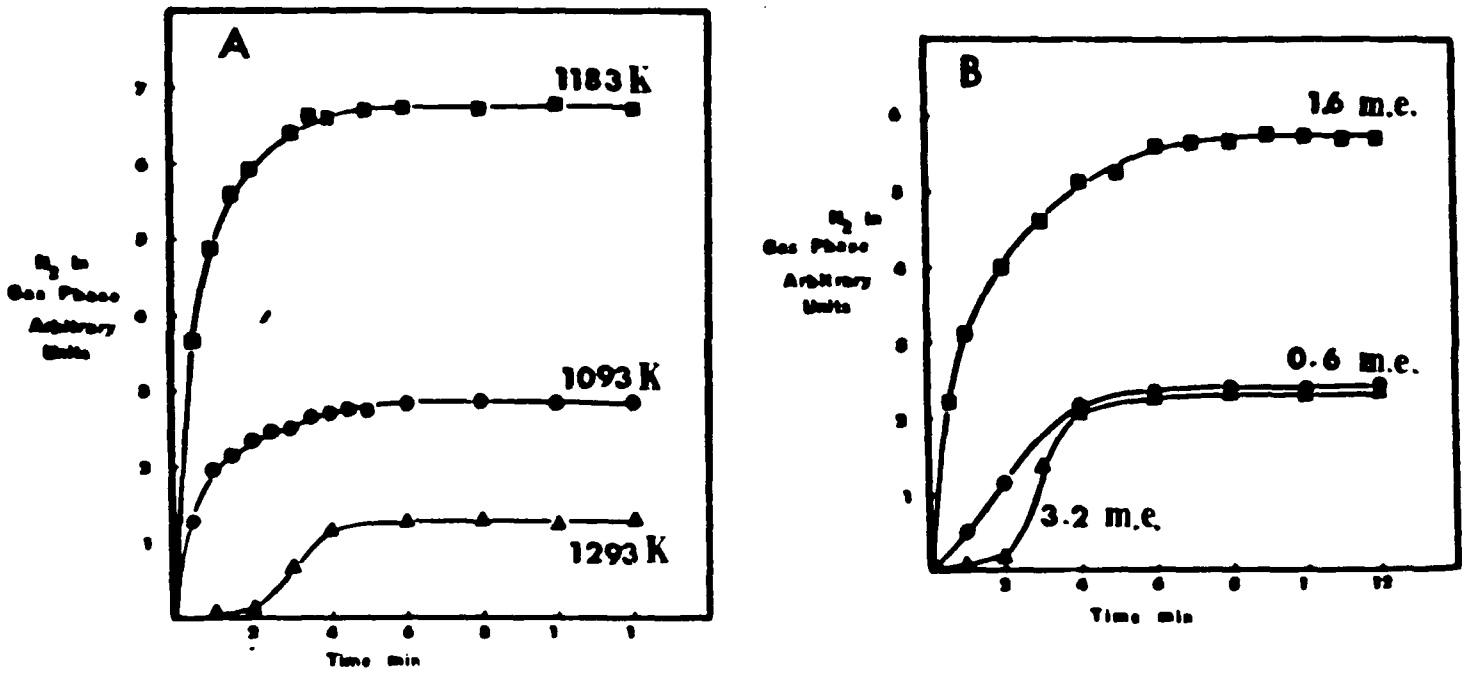

Figure B5. Build-up of N_2 product from N_2O dissociation at 300 K over Ba^{2+}/MgO samples in static reactor:

5A Relative rates of build-up over same 3.2 m.e. Ba^{2+}/MgO sample after preactivation at indicated temperatures.

5B Relative rates of build-up over different samples having indicated nominal surface loadings of Ba^{2+}. All samples similarly preactivated at 1273 K.

Evidence pointing to the importance of significant surface concentration of Ba^{2+} as a surface dopant, if activity for N_2O dissociation at 300 K was to be observable, came from comparisons of the activity of various samples subjected to identical preparation and preactivation in vacuo at 1273 K. These showed that, in marked contrast to Ba^{2+}/MgO samples, neither undoped MgO nor BaO yielded detectable decomposition of N_2O at 300 K. Figure 5B illustrates some results of a comparison between the relative activities of Ba^{2+}/MgO samples having different nominal loadings of Ba^{2+}. Maximum extent of decomposition was observed for the material with nominal loading of 1.5 m.e. which is close to where it could be expected on the basis of our working hypothesis, viz. at 1 m.e. when ca. 0.5 m.e. of Ba^{2+}_{cus} displaced outward by 1.21 lattice units (cf. Fig. 1), and resulting high possibility for localization of excess electrons in the proximity of some Ba^{2+}_{cus} sites, could be anticipated.

It was noted above that quenching of luminescence from Ba^{2+}/MgO by oxygen was fully reversible and indicative of only weak interaction at the O_2/Ba^{2+}/MgO interface. An electron-transfer initiated mechanism by which the R^O-type oxygen isotope exchange process of eqn. 2b can proceed at oxide surfaces via only weak interactions has been discussed elsewhere by one of the authors (ref. 15). That mechanism requires the availability of M^{2+}_{cus} surface locations and it was of interest to determine experimentally whether, and after what preactivation temperature, eqn. 2b would be enhanced at O_2/Ba^{2+}/MgO interfaces at 300 K. An enhancing effect of Ba^{2+} surface dopant was indeed found in respect of the relative room temperature activities of similarly preactivated samples of Ba^{2+}/MgO, MgO and BaO for the R^O-type oxygen isotope exchange process represented by eqn. 2b. Thus BaO surfaces developed significant activity only after outgassing for 6 h at 1293 K. Outgassing for at least 1 h at 1273 K was required to develop activity of the MgO material. However, appreciable

activity appeared for e m.e. Ba^{2+}/MgO following preactivation at only 900 K. Time to 50% equilibration of a 0.1 torr aliquot of ($^{16}O_2$ + $^{18}O_2$) decreased to ca. 25 sec after preactivation at 993, 1053 or 1153 K but then increased again. Such dependence upon preactivation temperature for Ba^{2+}/MgO contrasted with that noted for BaO and MgO but did resemble that found for N_2O dissociation over Ba^{2+}/MgO. That resemblance would, in the context of our working hypothesis for surface reconstruction, be explicable if the development of similar ne^-/Ba^{2+}_{cus} surface locations by moderate preactivation were required to make possible both eqn. 2a and 2b and if such locations were diminished in number or subject to some deactivation upon outgassing at 1273 K.

ACKNOWLEDGMENTS

Spectroscopic aspects of this study were greatly facilitated through arrangements made by the late Dr. A.J. Tench for use of equipment at A.E.R.E. Harwell. The work was supported in part (J.N. and J.C.) through funding under AFOSR Contract 83-0074.

REFERENCES (cited in Appendix B)

1. S. Coluccia, A.M. Deane and A.J. Tench
   (a) J. Chem. Soc. Faraday Trans. I., 74 (1978) 2913.
   (b) Proc. 6th Int. Cong. on Catalysis, London, 1976.

2. S. Coluccia, R.L. Segall and A.J. Tench
   J. Chem. Soc. Faraday Trans. I, 75 (1979) 1769.

3. S. Coluccia and A.J. Tench
   Proc. 7th Int. Cong. on Catalysis, Tokyo, 1980.

4. S. Coluccia and A.J. Tench
   J. Chem. Soc. Faraday Trans. I, 79 (1983) 1881.

5. S. Coluccia, A. Barton and A.J. Tench
   J. Chem. Soc. Faraday Trans. I, 77 (1981) 2203.

6. M. Che and A.J. Tench
   Advances in Catalysis, 32 (1983) 1.

7. A. Zecchina, M.G. Lofthouse and F.S. Stone
   J. Chem. Soc. Faraday Trans. I, 71 (1975) 1476.

8. A. Zecchina, M.G. Lofthouse and F.S. Stone
   J. Chem. Soc. Faraday Trans. I, 72 (1976) 2364.

9. E. Garrone, A. Zecchina and F.S. Stone
   Phil. Mag., 42 (198o) 683.

10. E.A. Colburn, J. Kendrick and W.C. Mackrodt
    Surface Science, 126 (1983) 550.

11. W.J. Daley
    J. Chem. Soc. Faraday Trans. I, 80 (1984) 1173.

12. (a) W.C. Mackrodt and R.F. Stewart
    J. Phys., C12 (1979) 431.
    (b) C.R.A. Catlow and W.C. Mackrodt
    in Computer Simulation of Solids (Eds. Catlow and W.C. Mackrodt) Springer, Berlin, 1982.
    (c) P.A. Tasker, E.A. Colburn and W.C. Mackrodt
    J. Am. Ceramic Soc., (In Press).

13. C.S. Vempati, P.W.M. Jacobs
    Cryst. Lat. and Amorph. Mat., 10, pp. 9-17 (1983).

14. J. Cunningham, J.J. Kelly and A.L. Penny
    J. Phys. Chem.,
    (a) 74 (1970) 1992.
    (b) 75 (1971) 617.

15. (a) J. Cunningham, in C.H. Bamford and C.F. Tipper (eds.)
    Comprehansive Chemical Kinetics, Vol. 19, ch. 3, Elsevier, Amsterdam, 1984.

15. (b) J. Cunningham and E.L. Goold
J. Chem. Soc. Faraday Trans., 77 (1981) 837.

16. M. Che, A.J. Tench, S. Coluccia and A. Zecchina
J. Chem. Soc. Faraday Trans. I, 72 (1976) 1553.

APPENDIX II

Surface Reactivity and Spectroscopy Compared for Alkaline Earth Oxides: Part 2, Dependences upon Temperature of Preactivation for SrO

by

John Nunan, John A. Cronin and Joseph Cunningham

(Department of Chemistry, University College, Cork, Ireland)

Published in

Journal of Chemical Society (London)
Faraday Transactions I (1985)

Surface Reactivity and Spectroscopy Compared for Alkaline Earth Oxides: Part 2, Dependences upon Temperature of Preactivation for SrO

John Nunan, John A. Cronin and Joseph Cunningham,
(Chemistry Department, University College, Cork, Ireland).

ABSTRACT

High surface area samples of strontium oxide, prepared by thermal decomposition of high purity $SrCO_3$ in vacuo, have been examined for their reactivity/catalytic activity towards molecular gas probes and for luminescence spectra. Temperature profiles are reported, as a function of prior outgassing temperature, for the development of room-temperature excitation and emission spectra. These are compared with temperature profiles for the development of room-temperature catalytic activity for R_o-type oxygen isotope exchange, $^{16}O_2 + {}^{18}O_2 \rightleftharpoons 2{}^{16}O{}^{18}O$, and for development of activity for nitrous oxide decomposition, at various temperatures. Consideration is given to interpretations of the results in terms of ions at co-ordinatively unsaturated surface locations, to the extent to which these are exposed after thermal activation at various temperatures, and to the involvement of point defects in the surface locations responsible for the various surface processes.

Introduction

Absorption features lying to the long wavelength side of their absorption edges, and attributable to the photogeneration of correlated electron-hole pairs within the lattice (i.e. 'bulk-excitons'), have been reported for single crystals of high-purity alkali halides (1,2) and for some alkaline earth oxides, (3,4). In terms of the tight binding approximation (generally considered applicable to these groups of highly ionic solids) such bulk-exciton transitions may be thought of as promoting an electron from an anion site enjoying full octahedral co-ordination onto a similarly co-ordinated adjacent cation site. Thus within the bulk of a perfect single crystal composed of M_{6c}^{2+} and O_{6c}^{2-} ions, the upward transition may be approximated by

(Eqn 1a) $\left[M_{6c}(ns^{0})^{2+},\ O_{6c}(2\overset{6}{p})^{2-} \right] \xrightarrow{h\nu} \left[M_{6c}(n\overset{1}{s})^{+},\ O_{6c}(2\overset{5}{p})^{-} \right]^{*}$

Excitions thereby photogenerated, whilst highly mobile throughout perfect lattices at very low temperatures, are subject to radiative and non-radiative decay in real systems at normal temperatures, usually with the nett overall effect equivalent to the reverse of eqn. 1a. Radiative decay can occur via the intermediacy of self-trapped (2b), defect-trapped (5a) or impurity-trapped excitons (5b) and studies of such photoluminescence (emission) can yield information on the nature of the luminescence centres (5a,6).

Spectroscopic observations reported in the present series of papers for the isostructural alkaline earth oxides, MgO, CaO, SrO and BaO relate, however, to other electronic transitions which are displaced to longer wavelength by 2-4eV relative to bulk-exciton transitions. These are most readily observable in samples of high surface area, such as powdered oxide samples prepared by thermal

decomposition of the corresponding carbonates or hydroxides in vacuo at high temperatures. Careful reflectance measurements, mainly by Stone et al., have revealed three partially resolved absorption features, which they denote by I, II and III respectively and which they interpret in terms of 'surface excitons', i.e. transitions analagous to Eq. 1a, except that the anion and/or cation sites involved are at surface locations and do not enjoy full octahedral co-ordination (7,8). According to the interpretation espoused by Stone et al., features II and III in the reflectance spectra are to be associated with photogeneration of surface excitons involving O^{2-} having only four-fold or three-fold co-ordination, e.g.

(Eqn. 1b) $\left[M_{\ell c}(ns^{o})^{2+},\ O_{4c}(2\overset{6}{p})^{2-}\right] \xrightarrow{h\nu_{II}} \left[M_{\ell c}(ns^{1})^{+},\ O_{4c}(2\overset{5}{p})^{-}\right]^{*}$

(Eqn. 1c) $\left[M_{\ell c}(ns^{o})^{2+},\ O_{3c}(2\overset{6}{p})^{2-}\right] \xrightarrow{h\nu_{III}} \left[M_{\ell c}(n\overset{1}{s})^{+},\ O_{3c}(2\overset{5}{p})^{-}\right]^{*}$

Variation of these transition energies for the different alkaline-earth oxide in accordance with the Mollwo-Ivey relation for localised excitons (8) lent support to the interpretation of features II and III in terms of localised surface excitons. However, the transition energies of feature I were observed to vary in similar fashion to freely diffusing excitons of the bulk and this has been assigned to photogeneration, as in Eqn. 1d, of surface excitons at surface locations involving oxide ions having five-fold co-ordination upon flat {100} terraces of the metal oxide. (The subscript ℓc denotes low but unspecified co-ordination).

(Eqn. 1d) $\left[M_{\ell c}(ns^{o})^{2+},\ O_{5c}(2\overset{6}{p})^{2-}\right] \xrightarrow{h\nu_{I}} \left[M_{\ell c}(n\overset{1}{s})^{+},\ O_{5c}(2\overset{5}{p})^{-}\right]^{*}$

Interpretations favouring step-edges or corners as the surface topographical features mainly responsible for the existance of anions (and to lesser degree cations) with four-fold or three-fold co-

ordination, have been strongly espoused, not only by Stone and co-workers on the basis of reflectance measurements, but also by Tench et al. (9) on the basis of luminescence.

Recently, Duley has advanced an interesting variation upon the idea that co-ordinatively unsaturated oxide ions are important in interpreting luminescence and absorption features of high surface area alkaline earth oxide powders (5a). According to Duley's model, luminescence emission from MgO and CaO involves a charge transfer type transition from an electronically excited state of O^{2-}_{lc} to the ground state of an adjacent F^{+}_{s} centre, as in eqn. 2.

(Eqn. 2) $(O^{2-}_{lc})^{*} \ldots . F^{+}_{s} \longrightarrow (O^{-}_{lc}) \ldots . F^{*}_{s} + h\nu$

An essential difference between this representation and those in equations 1a-1d is the recognition given to an important role of point defects at the surface (the defects of importance in eqn. 2 being F^{+}_{s} centres, consisting of vacant anion sites at the surface upon each of which a single electron has been localised). In another recent paper Duley has considered involvements of co-ordinatively unsaturated hydroxide ion in luminescence from MgO and $Mg(OH)_2$ powders at various stages of hydration/dehydration (5c).

A preliminary account has recently been given (10) of marked effects of Ba^{2+} dopant upon surface processes on MgO and of a probable influence of surface reconstruction/relaxation in modifying the degree of co-ordination of surface ions. A brief account was also given therein of problems which attach to interpretation of surface processes mainly in terms of ions at unrelaxed step, edge or corner locations. In view of these additional influences upon surface luminescence from alkaline earth oxide powders - and particularly of

the very differing emphases possible for surface defects and surface impurities - we have initiated a programme to examine the extent of correlation between surface luminescence and other surface properties likely to be dependent upon surface concentrations of point defects or impurities (10). Surface reactivity, and catalytic activity for gaseous reactions mediated by charge transfer were selected as appropriate defect-sensitive processes. Furthermore, in view of the reported dependences of the surface reactivity and catalytic activity of alkaline earth oxide powders (11-15) upon temperatures of prior activation, an important element of the strategy adopted in this second paper of the series is a careful comparison, made throughout with the same SrO material, between the dependences exhibited by surface luminescence and surface catalytic activity upon temperature of prior activation.

Experimental

Vacuum Procedures: Both the thermal decomposition of strontium carbonate to SrO and its subsequent activity for N_2O decomposition, or for the homomolecular oxygen isotope exchange (i.e. process, $O_2^{16} + O_2^{18} \rightarrow 2O^{16}O^{18}$), were studied in a static quartz reactor using conventional vacuum procedures (base pressure 5×10^{-6} torr) with mass spectrometric analysis (base pressure 10^{-8} torr). In order to follow the progress of the thermal decomposition of high purity $SrCO_3$ ('Spex' spectroscopically pure grade) in the quartz reactor, a powdered sample was slowly heated to 1273K over a period of ten hours during which the total pressure was monitored and the composition of gaseous decomposition products determined by leaking samples to a VG Micro Mass 6

mass spectrometer via a leak valve. Progress of thermal decomposition during activation in vacuo at temperatures up to 1273 K was also monitored by taking IR spectra at 300 K - after periods of activation at high temperature - upon thin self-supporting discs, initially fabricated from $SrCO_3$ but converted progressively to SrO.

Nitrous oxide was supplied by B.D.H. Chemicals and had a purity of greater than 99%. Before contacting $P_{N_2O} \simeq 3.5$ torr with the catalyst, the gas was further purified by a series of freeze-pump-thaw cycles, after which purity was further checked by leaking the gas into the spectrometer through a by-pass valve. With the SrO catalyst at temperatures in the range 673 - 873K, reaction was initiated by admitting purified N_2O and periodically obtaining the mass spectrum of gas samples leaked into the spectrometer. Reaction temperature and catalyst mass were chosen such that the reaction time for 50% conversion was greater than ten minutes. Under these conditions the reaction rate was found not to be limited by diffusional effects.

For oxygen isotopic exchange studies, an isotopically non-equilibrated mixture, consisting of 50% O_2^{16} + 50% O_2^{18}, was employed (Norsk Hydro). This gas was contacted with the catalyst at room temperature. The mass spectrometric procedure was the same as for N_2O decomposition, but oxygen pressures in the range 0.1 to 0.01 torr were used. In general SrO was activated prior to reaction by heating under vacuum to the required activation temperature and maintaining this temperature for one hour before cooling to room temperature in vacuo. Base pressure in the vacuum system employed was 5×10^{-6} torr.

Gas Chromatographic Procedures: Nitrous oxide decomposition was also studied using g.l.c. and microcatalytic, flow-reactor systems

operating at atmospheric pressure. A feature of these studies was the use of both the continuous flow and pulsed-reactant procedures and full details have elsewhere been given illustrating use in both modes (16). Strontium carbonate samples (200 mg) were decomposed in-situ in the quartz microcatalytic reactor by heating at different temperatures, up to a maximum of 1273 K, for one hour in a flow of dry helium at a flow rate of 40 mls. per minute. Prior to the admission of nitrous oxide as pulses, or as a continuous flow, the catalyst temperature was lowered to the reaction temperature in the flow of pure dry helium. The reactor was then isolated while N_2O/He mixtures were prepared such that the pressure of N_2O took values in the range 50 to 250 torr. The total flow rate was then restored to 40 mls. per minute.

Luminescence Procedures: Instrumentation used in obtaining the excitation/emission spectra has previously been described in detail (9). Excitation was provided by a 250 W Xenon lamp from which appropriate wavelengths were sequentially selected, using two Spex f4 monochromators whilst taking excitation spectra. Another Spex monochromator, placed between sample and detector, was held at a fixed wavelength and augmented by appropriate cut-off filters in taking excitation spectra. Spectra were automatically corrected for variations in excitation intensity with time, or changing wavelength, via instrumental comparisons (with an Ortec photon-counting system) of the pulse rates from two photomultipliers: one monitoring luminescence intensity and the other the intensity of the source at the same wavelength. Excitation spectra at acceptable signal/noise ratio were only obtained upward from 230 nm due to low source intensity at shorter wavelengths. In taking emission spectra under

excitation at fixed wavelength, sharp cut-off filters (Corning 3-74 and 0-52) were placed between the sample and the emission monochromator to minimise scattered wavelengths from the Xenon source reaching the photomultiplier. A band-pass of 5 nm was used for both the excitation and emission results.

RESULTS

1. Sample Activation

Decomposition profiles of $SrCO_3$ as a function of the outgassing temperature are summarised in Figure 1. Use of total pressure of gaseous products as the monitor (cf. plot S_3) indicated that the carbonate started to decompose at 873 K, reached a maximum at 1023 K and was almost complete at 1073 K. Mass spectrometric analysis shows that the major decomposition products were CO_2 and CO, as shown by plot S_1 of Figure 1, but some water vapour was also present. As indicated by plot S_2 of the figure, the ratio of CO/CO_2 changed markedly as the activation temperature was increased above 1073 K, with CO becoming the dominant decomposition product at the higher temperatures (cf. Fig. 1c), presumably due to onset of a dissociation of residual surface CO_2 upon sites exposed at the higher temperatures.

Progress of the thermal decomposition of $SrCO_3$ and its conversion to SrO can also be discerned from Figure 2, which presents a summary of IR spectra obtained at 300 K from a self-supporting disc, following activation in vacuo at the indicated temperatures. Clearly evident therein is the progressive diminution of IR bands (2400, 1780, 1090 cm^{-1}) characteristic of bulk CO_3^{2-} and conversely the appearance of bands (1000-800 cm^{-1}) characteristic of bulk oxide (17a). Particular interest attaches, however, to the temperature needed for total

removal of bands at 1090 cm^{-1} and 1460 cm^{-1} which previous workers have identified with CO_3^{2-} in the aragonite stucture (17b). Our observation that these were not totally removed until vacuum outgassing reached 1173 K make it necessary to take into account the persistence of some $SrCO_3$ - like regions to considerably higher temperatures than might be suggested (ca. 1073 K) by the mass spectrometric data in Fig. 1. Another significant feature of the IR studies, which is not depicted in Fig. 2, was the lack of evidence to indicate extensive hydroxylation at any of the stages represented on Fig. 2.

Effects of prior outgassing at different temperatures on the emission/excitation spectra of SrO at room temperature are shown in Figure 3. The excitation/emission spectra appeared only upon outgassing above 1073K, which Fig. 1 showed to correspond to decomposition of the bulk carbonate. Further increases in outgassing temperature brought about a progressive increase in the emission peak intensity and an accompanying increase in excitation peak intensity which Fig. 2 would suggest to coincide with removal of the last traces of CO_3^{2-}. Increasing the outgassing temperature also brought about significant changes in the peak shape and position. Thus in the excitation spectra, both a peak at 280 nm and an accompanying shoulder at 315 nm were observed to grow and experience changes in relative intensity in going from 1073 to 1273 K (cf. Figure 3A, plots (i), (ii), (iii) and (iv)). Upon outgassing for 4.0 hours at 1293 K the relative intensity in the latter shoulder was observed to decrease again (cf. Fig. 3A(v)). Parallel observations upon the emission spectra of the same sample showed that outgassing at 1123K led to two broad peaks centered at 400 and 455 nm (cf. Figure 3B(11)). Outgassing at the higher

temperature of 1173, 1223 and 1273K resulted in a single peak at 465 nm, as shown in Figure 3B, plots (iii) and (iv). However, extensive outgassing at 1293K for 4.0 hours led to a shift in the emission maximum back to 450 nm and a reduction in its intensity of ca. 40% (plot (v) Fig. 3B).

Figure 4 illustrates the effects of exciting the emission at different excitation wavelengths for a SrO sample first outgassed at 1123 and then at 1293K. It is clear that for the sample pre-treated in these different fashions, the emission peak shape and position remained independent of the exciting wavelength. This was also found to be the case for samples outgassed at 1173, 1223 and 1273K.

These excitation and emission results agree well with those reported by Coluccia et al. (9b). In excitation the band having max at 280 nm, similar to that previously attributed by Coluccia to five-co-ordinate surface positions, appeared first. The other weaker band with max at 315 nm, similar to that attributed by Coluccia to four-coordinate surfaces locations, only developed as outgassing temperature increased towards 1273K. In emission, the bands shown in Fig. 3B as the first to develop in our spectra with max at 400 and 450 nm, are very similar to those assigned by Coluccia to emission from surface locations involving five-fold and four-fold co-ordination respectively. The development of emission with max at 465 nm only after outgassing at the higher temperatures, as illustrated by Fig. 3B iii, had previously been interpreted in terms of the involvement of surface ions with three-fold co-ordination. Furthermore, our observation that, regardless of whether excitation of SrO outgassed at the higher temperatures was made at 280 or 315 nm, emission was dominated by the

band at 450 nm reproduces observations made earlier by Coluccia et al. and attributed by them to energy transfer from sites of five-fold co-ordination (excited by photons having λ = 280 nm but emitting at 400 nm) to sites of four-fold co-ordination (excited by photons having λ= 315 nm but emitting at 450 nm). It was encouraging that our observations upon the spectral parameters of luminescence were qualitatively so similar to those of Colluccia et al., despite differences in starting materials and steps for its conversion to SrO. However, details of the dependence of luminescence upon temperature of sample outgassing, which are also contained within Figures 3-5, will - when compared with temperature dependence of surface reactivity/catalytic activity (see below) - serve to call into question the adequacy of relying upon varying relative exposures of O^{2-}_{3c}, O^{2-}_{4c} and O^{2-}_{5c} as the sole arbitrer of surface properties.

3. Surface Reactivity

The stoichiometry of the nitrous oxide decomposition at reaction temperatures 673 - 873 K over SrO samples pretreated in the ways indicated in the experimental section agreed within experimental error with the equation:

$$N_2O_{(g)} \longrightarrow N_{2(g)} + {}^1/_2O_{2(g)} \qquad \text{(Eqn. 3)}$$

The reaction exhibited first-order kinetics, whether studied by the mass spectrometric (m.s.) procedure or by the gas chromatographic (g.c.) procedure. In Figure 5A are shown the first-order plots of N_2O decomposition at 627, 656 and 683 K obtained using mass spectrometry. Linear regressison analysis gave correlation co-efficients ranging from 0.992 to 0.997 for the three plots. In the gas chromatographic

continuous-flow studies, kinetic data were obtained under conditions where the reactor was operating in the differential mode. This was achieved by selecting the reaction-temperature, catalyst-mass and flow-conditions such that the conversions were less than 4%. Plots of the reciprocal space velocity versus conversion within this range were found to be linear, as shown by the insert on Fig. 5B. Consequently the percentage conversion gives a direct measure of the rate of reaction. Applying the method of plotting of log Rate vs. Log P_{N_2O}, the reaction was shown to be first order with respect to N_2O pressure in the pressure range 50 ot 250 torr, as illustrated in Figure 5B. In this manner first-order kinetics in N_2O decomposition were shown to be obeyed over SrO (ex$SrCO_3$) preactivated at various temperatures in the temperatures range 773 to 1273 K, independent of whether the reaction was studied using m.s. or g.c. procedures.

The effect of outgassing temperature on the reaction rate is summarised in Figure 6 where the first-order rate constants obtained using g.c. are plotted versus outgassing temperature. It is evident from Figure 6 that, while some steady-state activity for N_2O decomposition became apparent after outgassing at 900 K, the rate only began to increase rapidly after outgassing at temperatures >1073, i.e. in the range where Fig. 2 indicated removal of residual traces of CO_3^{2-}.

The use of the gas chromatographic procedure in its pulsed-reactant mode allowed investigations to be made of any progressive changes brought about in sample activity by contacting a preactivated SrO sample with a succession of individual pulses of nitrous oxide. In this way low exposure activity profiles (l.e.a.p.) of surface

activity could be developed. Figure 7 shows how such l.e.a.p. plots varied with increasing pulse number (each pulse ~4 x 10^{-7} mole of N_2O) for different temperatures. Comparison of the three l.e.a.p. profiles, all measured at identical reaction temperature, demonstrate two important points: firstly, the activity maximum attained in a profile was lowest after preactivation in vacuo at 993K and was increased by increased preactivation temperature; and secondly that, although the drop-off in activity after the maximum was quite abrupt for samples preactivated at 993K or 1083K (so that activity declined rapidly towards zero after a small number of pulses), no such abrupt drop-off in activity was found for the sample preactivated at 1273K. Rather the activity for N_2O decomposition continued at a high level up to large pulse numbers when the sample had been preactivated at this high temperature. The first of these points agree well with existing hypotheses that the level of surface activity depends upon the extent to which more highly co-ordinatively unsaturated surface ions are exposed/developed at progressively higher preactivation temperatures. An adequate explanation of the second point requires some extension/modification of existing hypotheses which is attempted in the Discussion. Such extension/modifications will also be relevant to observations made upon the ratio of N_2 to O_2 products from N_2O pulses delivered in the experiments depicted in Fig. 7. These showed that, whilst at any of the selected temperatures the N_2/O_2 product ratio did not vary significantly with pulse number, the ratio took the very different values of 2.0, 3.0 and 3.8 during sequences of pulses introduced for samples previously outgassed at 993, 1083 and 1273 K, respectively.

Oxygen isotope exchange was studied using Mass Spectrometry (18). After preactivation of the SrO (ex $SrCO_3$) samples at adequate temperatures the reaction occurred readily at room temperature. This is illustrated in Figure 8 where the mole fractions of $^{16}O_2$, $^{16}O^{18}O$ and $^{18}O_2$ viz, X_{32}, X_{34} and X_{36} respectively, are plotted as a function of time. During the course of the reaction the atom-fractions of ^{16}O and ^{18}O remained constant in the gas phase, thus indicating that an R_o type isotopic exchange process was occurring, i.e.

$$^{16}O_{2(g)} + {}^{18}O_{2(g)} \rightleftharpoons {}^{16}O^{18}O_{(g)} \qquad \text{(Eqn. 4)}$$

without significant accompaniment of an R_1 or R_2-type exchange with lattice oxygen-16.

Effect of temperature of prior activation upon the level of activity for R_o-type o.i.e. subsequently measured at room temperature is clearly shown in plot (ii) of Fig. 9. There the reciprocal of , the time required for surface-assisted movement by 50% towards total equilibration, is used as a measure of rate of the isotopic equilibration process and is plotted as a function of prior outgassing temperature. For a constant preactivation period of 1 hr. at each temperature, plot (ii) of Fig. 9 indicates a rather sharp onset of activity after outgassing at 1023 K, followed by an essentially linear increase for higher outgassing temperatures. Plot (i) of Fig. 9 represents for purposes of comparison the dependence upon temperature of preactivation observed in a related set of experiments wherein magnitude of the first-order rate constant for N_2O decomposition at 758 K was determined after 1 hr. preactivation of the Sr-O at various temperatures. Although the same static reactor and mass spectrometric method of analysis were employed for both sets of experiments, it is

clear that the onset of activity is more sharply defined for the o.i.e. plot and that its initial slope is much steeper than for N_2O decomposition.

DISCUSSION

The foregoing results evidence considerable success in the search for similarities between dependences upon temperature of prior activation in the development of surface photoluminescnece and of surface reactivity. Such correlation is most direct in the case of the R_o-type oxygen isotope exchange reaction (o.i.e.), since surface luminescence and surface activity were both measured in similar condition, i.e. at room temperature after cooling down from the higher preactivation temperatures. Furthermore, it is well established from previous reports of quenching of the surface luminescence by molecular oxygen that (7-9) O_2 species interact reversibly at 300 K with the centres responsible for luminescence, even at the low pressures (10^{-1} to 10^{-2} torr) employed in obtaining surface reactivity data such as shown in Fig. 8. The fact that the temperature profile for development of o.i.e. activity (cf. plot II of Fig. 9) rises rapidly across the same temperature range (1073-1273 K) as was required for rapid enhancement of surface luminescence thus provides good support for the idea that a relationship exists between sites involved in surface photoluminescence and those conferring catalytic activity for o.i.e. in accordance with Eqn.4 It has been deduced from previous studies of the latter process upon ZnO surfaces (18,19): (a) that the catalytically active sites involve surface cations at locations of high co-ordinative unsaturation; and (b) that the ready availability of at least one

electron from a shallow energy level or trap in the immediate vicinity of the (M^{2+}_{cus}) locations is also necessary to trigger o.i.e. thereon (via an electron-transfer-catalysed chain reaction requiring negligible energy of activation). Both of these requirements seem likely to be satisfied by the ($O^{2-}_{\ell c}$ ... F^{+}_{s}) surface locations proposed by Duley (5a) as being responsible for surface luminecence from high surface area MgO and CaO, since: (a) the Sr^{2+} cations involved in the F^{+}_{s} point defect necessarily have at least two degrees of co-ordination unsaturation, and (b) relatively low energies can be expected for transfer of an electron from a ground state $O^{2-}_{\ell c}$ to an adjacent F^{+}_{s}. Thus, according to Duley's interpretation such transfer is responsible for a broad absorption centered upon 2eV and detectable in MgO previously exposed to high energy radiations in vacuo. Still lower energy could be expected for thermal, rather than optical, promotion of an electron from O^{2-}_{c} to an adjacent F^{+}_{s} for MgO. Further reductions in energy could be anticipated for SrO relative to MgO, and for (O^{2-}_{c} ... F^{2+}_{s}) locations relative to ($O^{2-}_{\ell c}$ ... F^{+}_{s}). Thus it is reasonable to envisage o.i.e. upon SrO proceeding, in analagous fashion to that previously detected for ZnO surfaces, via activation of oxygen under the combined influence of a readily available electron and co-ordinatively unsaturated cation(s). Viewed in this context the experimentally observed dependence of the extent of room-temperature o.i.e. activity of the SrO (ex $SrCO_3$) surfaces upon temperature of prior activation (cf. plot ii of Fig. 9), should reflect the increase in number of ($O^{2-}_{\ell c}$ ... F^{n+}_{s}) surface locations with preactivation temperature (n = 1 or 2).

The exact implications of the good agreement with first-order kinetics here observed (cf. figure 5A and 5B) for ongoing decomposition

of N_2O at 758 K clearly depend upon the mechanism of the metal-oxide assisted decomposition, and in particular upon which step is the rate determining process (r.d.p.). Electron transfer from active sites on the metal oxide surface to N_2O adsorbate has been proposed (20,21) by many workers as the initial step (cf. eqn. 5a below). However, the rate-determining role has often been assigned rather to a step by which the necessary reverse electron-transfer is accomplished (22). We may denote these electron transfer processes respectively by

$$N_2O_{(ads)} + e^-/D_s/ \longrightarrow N_2O^-_{(ads)} \longrightarrow N_{2(g)} + O^-_{(ads)}/D_s/ \quad .... \quad (5a)$$

followed by

$$O^-/D_s/ + N_2O_{(g)} \rightarrow N_{2(g)} + O_2 + e^-/D_s/ \quad .... \quad (5b)$$

Note the adoption at this stage of the non-commital notation, $/D_s/$, for surface locations with which an electron or an oxygen fragment can be loosely associated (as in $e^-/D_s/$ and $O^-/D_s/$ respectively) and which are envisaged to play important roles in N_2O decomposition. However, the ability of such a two-step mechanism to account for the observations upon pseudo steady-state rate of N_2O decomposition in the continuous-flow mode is largely independent of the nature of $/D_s/$. Thus the operation of step 5b as the slow r.d.p. in conditions such that available D_s sites were effectively saturated by O^-, would account for first-order dependence upon P_{N_2O}. Furthermore, the experimentally observed dependence of the pseudo steady-state rate of decomposition upon the temperature of preactivation (cf. Fig. 6) may be understood to arise because the available surface concentration of the entity $O^-/D_s/$ in 5b, was predetermined by the surface concentration, θ_{D_s}, of active sites developed by prior activation. In the context of this two-step mechanism and of the similarities between the experimentally

observed profiles for development of activity for N_2O dissociation and oxygen isotope exchange (cf. Fig. 9), it is of interest to consider whether the $e^-/D_s/$ sites envisaged in Eqn. 5a may be similar to the $(O^{2-}_{\ell c} \ldots F^+_s)$ locations favoured earlier as the active sites for o.i.e. on SrO. At first glance, the fact that the profiles in Fig. 9 do not reveal three distinguishable segments-corresponding to temperature regimes dominated respectively by the growth of O^{2-}_{5c}, O^{2-}_{4c} and O^{2-}_{3c} as envisaged by others in temperature profiles for development of photo luminescence features - might be construed as an argument against equating $e^-/D_s/$ with the $(O^{2-}_{5c} \ldots F^+_s)$, $(O^{2-}_{4c} \ldots F^+_s)$ and $(O^{2-}_{3c} \ldots F^+_s)$ situations envisaged by Duley. However, an alternative interpretation which cannot be overruled and which would permit equivalence between $e^-/D_s/$ and $(O^{2-}_{\ell c} \ldots F^+_s)$ sites, is that the electron transfer required to initiate N_2O dissociation (cf. Eqn. 5a) or o.i.e. (cf. Ref[8-20]) can occur to adsorbed reactant with comparable facility from $(O^{2-}_{5c} \ldots F^+_s)$, $(O^{2-}_{4c} \ldots F^+_s)$ and $(O^{2-}_{3c} \ldots F^+_s)$ locations, thereby rendering molecular probes incapable of distinguishing between such locations. In such a situation, differences between the degree of detail revealed respectively by temperature profiles for development of surface activity and of surface photoluminescence would not only be allowed but even expected.

The value observed experimentally for the ratio N_2/O_2 (between gaseous N_2 and O_2 products detected as well-formed peaks in the g.c. technique) represents a further criterion for agreement/disagreement with a mechanism involving 5a and 5b. Thus the value of 2.0 observed for this ratio in the continuous-flow conditions under P_{N_2O} from 50 to 380 torr, agreed well with the mechanism. Recall, however, the very significant upward deviation of this ratio observed in the pulsed reactant mode whenever the temperature of preactivation of SrO

was progressively increased (ratio values of 2.0, 3.0 and 3.8 after preactivation at 993, 1083 and 1273 K respectively). Such deviation would be consistent with enhanced competition, under the conditions prevailing in the pulsed reactant mode, between the foregoing two-step mechanism having 5b as the slow oxygen-producing step and another process which instead incorporated fragments from N_2O decomposition into the oxide surface. Likely processes of the latter type are represented in equations 6a and 6b, which respectively involve incorporation of an oxygen fragment from N_2O into an anion vacancy doubly-occupied by electrons, $2e^-/\square_s/$, or by surface groupings of m low co-ordinate cations . .

$$N_2O_{(g)} + 2e^-/\square_s/ \longrightarrow N_2(g) + O_s^{2-} \qquad 6(a)$$

$$N_2O(g) + mSr_{\ell c}^{2+} \longrightarrow N_2(g) + O/mSr_{\ell c}^{2+}/ \qquad 6(b)$$

Some approach towards equilibrium concentrations of point defects at the surfaces is thermodynamically to be expected during the preactivation treatments, greater concentration being expected during preactivation at higher temperature . A "freezing-in" of some fraction of such defect concentrations during the rapid cool-down to 758 K would result in significant probability of 6a and/or 6b upon contact with the initial pulses of N_2O admitted in the pulsed reactant mode. The extent to which this could drive the N_2/O_2 ratio during l.e.a.p. plots away from the value of 2.0 expected if only 5a and 5b were significant ould, as observed in the pulsed-reactant experiments, be greater after greater temperature of preactivation due to freezing-in of a greater number of defects. For the continuous-flow conditions only a low survival probability would be expected for such defects after the much higher integrated exposures (typically 2×10^6 torr sec) to N_2O which preceded measurement of steady-state activity for N_2O decomposit-

ion. This would account for the negligible deviation of the N_2/O_2 ratio from 2.0 in the continuous-flow mode regardless of the sample temperature during preactivation. Deviation of the ratio from 2.0 during determination of l.e.a.p. plots, with extent of deviation observed to increase with temperature of prior activation, contrasts with those steady-state Results and points to an important role of surface defects at the SrO surface at low exposures.

ACKNOWLEDGEMENTS

This work was supported by the U.S. Air Force Office of Scientific Research under Grants AFOSR 82-0023 and 83-0074. The authors are also grateful to the Department of Education of the Irish Government and to University College, Cork, for support (JAC).

REFERENCES

1. (a) J.E. Ely, K.J. Tergarden and D.B. Dutton, *Phys. Rev.*, (1959), 116, 1099; (b) W.H. Hamill, *Phys. Rev.*, 1969, 185, 1182.
2. (a) D.L. Dexter and R.S. Knox, *Excitons*, Interscience Publishers, 1965; (b) T. Higashimura, Y. Nukaoka and T. Iida, *J. Phys. C. Solid State Phys.*, 1984, 17, 4127.
3. B. Henderson and J.E. Wertz, *Adv. Physics*, 1978, 17, 749.
4. V.M. Bermudez, *Prog. Surf. Sci.*, 1981, 11, 1.
5. (a) W.W. Duley, *Phil. Mag. B.*, 1984, 49, 159; (b) K. Teegarden in *Luminescence of Inorganic Solids*, ed., P. Goldberg, Academic Press, New York, 1966.
6. R.C. Whitel and W.C. Walker, *Phys. Rev.*, 1969, 188, 1380.
7. A. Zecchina, M.G. Lofthouse and F.S. Stone, *J. Chem. Soc. Faraday Trans I*, 1975, 71, 1476.
8. E. Garrone, A. Zecchina and F.S. Stone, *Phil. May.*, 1980, B42, 683.
9. (a) A.J. Tench and G.T. Pott, *Chem. Phys Lett.*, 1974, 26, 59a; (b) S. Collucia, A.M. Deane, A.J. Tench, *J. Chem. Soc. Faraday Trans I*, 1978, 74, 2913; (c) S. Collucia and A.J. Tench, *loc. cit.*, 1983, 79, 1881.
10. J. Nunan, J. Cunningham, A.M. Deane, E.A. Colbourn and W.C. Mackrodt in *Adsorption and Catalysis on Oxide Surfaces*, eds. M. Che and G. Bond, Elsevier, 1984 (in press).
11. (a) D. Cordischi, V. Indovina and M. Occhiuzzi, *J. Chem. Soc. Faraday Trans. I*, 1978, 74, 456; (b) V. Indovina and D. Cordischi, *loc. cit.*, 1982, 78, 1705.
12. (a) M.J. Baird and J.H. Lunsford, *J. Catal.*, 1972, 26, 440; (b) Y. Tanaka, H. Hattori and K. Tanaka, *Chem. Lett.*, 1976, 37.
13. (a) H. Hattori and A. Satoh, *J. Catal.*, 1976, 45, 32; (b) M. Mohri, K. Tanabe and H. Hattori, *J. Catal.*, 1974, 32, 144.
14. (a) H. Hattori, K. Marayama and K. Tanabe, *J. Catal.*, 1976, 44, 50; (b) M. Mohri, H. Hattori and K. Tanabe, *J. Catal.*, 1974, 32, 144.

15. (a) L. Parrot, J.W. Rogers, Jr., and J.M. White, *Appl. Surf. Ser.*, 1978, 1, 443; (b) H. Noeller and K. Thomke, *J. Mol. Catal.*, 1979, 6, 375.

16. J. Cunningham, B.K. Hodnett, M. Ilyas, J.P. Tobin and E.L. Leahy, *Faraday Discuss Chem. Soc.*, 1981, 72, 283.

17. (a) K. Nakamoto, *Infrared and Raman Spectra of Inorganic and Coordination Compounds*, 3rd ed., Wiley Interscience, New York, 1978; (b) S. Pinchas and I. Ilaalicht, *Infrared Spectra of Labelled Compounds*, Academic Press, 1971, p.

18. (a) J. Cunningham and E.L. Goold, *J. Chem. Soc. Faraday Trans. I*, 1981, 77, 837; (b) J. Cunningham, E.L. Goold and J.L.G. Fields, *loc. cit.*, 1982, 78, 785.

19. J. Cunningham in *Comprehensive Chemical Kinetics*, vol. 19, (eds. C.F. Tipper and C.H. Bamford), Elsevier, Amsterdam, 1984, p. 362.

20. J. Cunningham, J.J. Kelly and A.L. Penny, *J. Chem. Soc. Faraday Trans. I*; (a) 1970, 74, 1992; (b) 1971, 75, 617.

21. N.B. Wong, Ben Taarit and J.H. Lunsford, *J. Chem. Phys.*, 1974, 60, 2149.

22. (a) F.S. Stone, *J. Solid State Chem.*, 1975, 12, 271; (b) G. Blyholder, *J. Phys. Chem.*, 1971, 75, 1037.

LEGENDS TO FIGURES

Figure 1 Mass spectrometric observations upon the $SrCO_3 \rightarrow SrO$ conversion in vacuo as a function of outgassing temperature. The total pressure of gaseous decomposition products is shown in S_3; S_1 shows combined peak heights of ($CO + CO_2$); the ratio of CO/CO_2 peak heights is given in S_2.

Figure 2 IR (at 300 K) of $SrCO_3 \rightarrow SrO$ conversion after vacuum outgassing respectively at: 293 K (A), 973 K (B), 1073 K (C), 1173 K (D) each for 1 hour.

Figure 3 Excitation spectra (Fig. 3A) and emission spectra (Fig. 3b) of high surface area strontium oxide obtained by outgassing $SrCO_3$ at various temperatures from 1073 to 1293 K: A(i) and B(i) excitation and emission spectra respectively from SrO outgassing for one hour at 1073 K; A(ii) and B(ii) spectra after outgassing for one hour at 1123 K; A(iii) and B(iii) spectra after outgassing at 1123 K for one hour; A(iv) and B(iv) spectra after outgassing at 1173/1273 K for one hour; A(v) and B(v) spectra after outgassing at 1293 K for four hours.

Figure 4 Emission spectra of $SrCO_3$ excited by different wavelengths of exciting light after outgassing at 1073 (Fig. 4A) and 1293 K (Fig. 4B): plots A(i) and B(i) are emission spectra observed under excitation at λ = 280 nm from SrO outgassed

at 1073 and 1273 K respectively; A(ii) and B(ii) emission spectra excited at λ = 299 nm from SrO outgassed at 1073 and 1273 K respectively; A(iii) and B(iii) emision spectra excited at λ = 315 nm from SrO outgassed at 1073 and 1293 K respectively; B(iv) emission spectra excited at λ = 325 nm from SrO outgassed for one hour at 1173/1293 K.

Figure 5 Evidence from Kinetic analysis for FIRST ORDER character of N_2O decomposition at 700 $\pm$ 50 K following preactivation of the SrO material at higher temperatures: (5A) First order plots of data obtained by mass spectrometric monitoring of N_2O decomposition in a static reactor over SrO preactivated at 1133 K: P_{N_2O} (initial) = 2.5 torr, reaction temperatures as indicated; (5B) Plot of Ln Rate vs. Ln P_{N_2O} for steady-state decomposition in a continuous flow reactor operated in the differential mode at 758 K over SrO preactivated at 1273 K for 6 hr. in an argon flow; Insert on 5B shows plot of steady state conversion vs. reciprocal space velocity at 740 K over sample similar to that in 5B.

Figure 6 Influence of temperature of prior activation of SrO samples upon the steady-state rate of N_2O decomposition at 758 K in the continuous flow G.C. procedure with input P_{N_2O} = 380 torr.

Figure 7 Low exposure activity profiles (l.e.a.p.) of SrO samples, obtained by measuring in the pulsed-reactant G.C. procedure, the extent of non-steady-state N_2O decomposition at 758 K for each of a succession of individual pulses (P_{N_2O} = 40 torr). The three profiles were obtained for SrO samples preactivated at three different temperatures, 993, 1083 and 1273 K.

Figure 8 Progress of the R_o-type oxygen isotope equilibration process at room temperature upon admitting an isotopically non-equilibrated equimolar mixture of $^{16}O_2$ plus $^{18}O_2$ into contact with an SrO sample preactivated in vacuo at 1223 K. Plots show the mole fraction of $^{16}O_2$ (X^{32}) and $^{18}O_2$ (X^{36}) decreasing with time (data points) and the mole fraction of $^{16}O^{18}O$ (X^{34}) increasing in agreement with Eqn. 4.

Figure 9 Influence of temperature of prior activation of SrO samples upon the rates of N_2O decomposition (plot I) and of R_o-type oxygen isotope exchange (plot II) as monitored by mass spectrometry. The kinetic parameters utilised as measure of the rates of the processes were, respectively, slopes of plots similar to those in Fig. 5A, and the time to 50% equilibration in plots similar to those in Fig. 8.

Fig.1

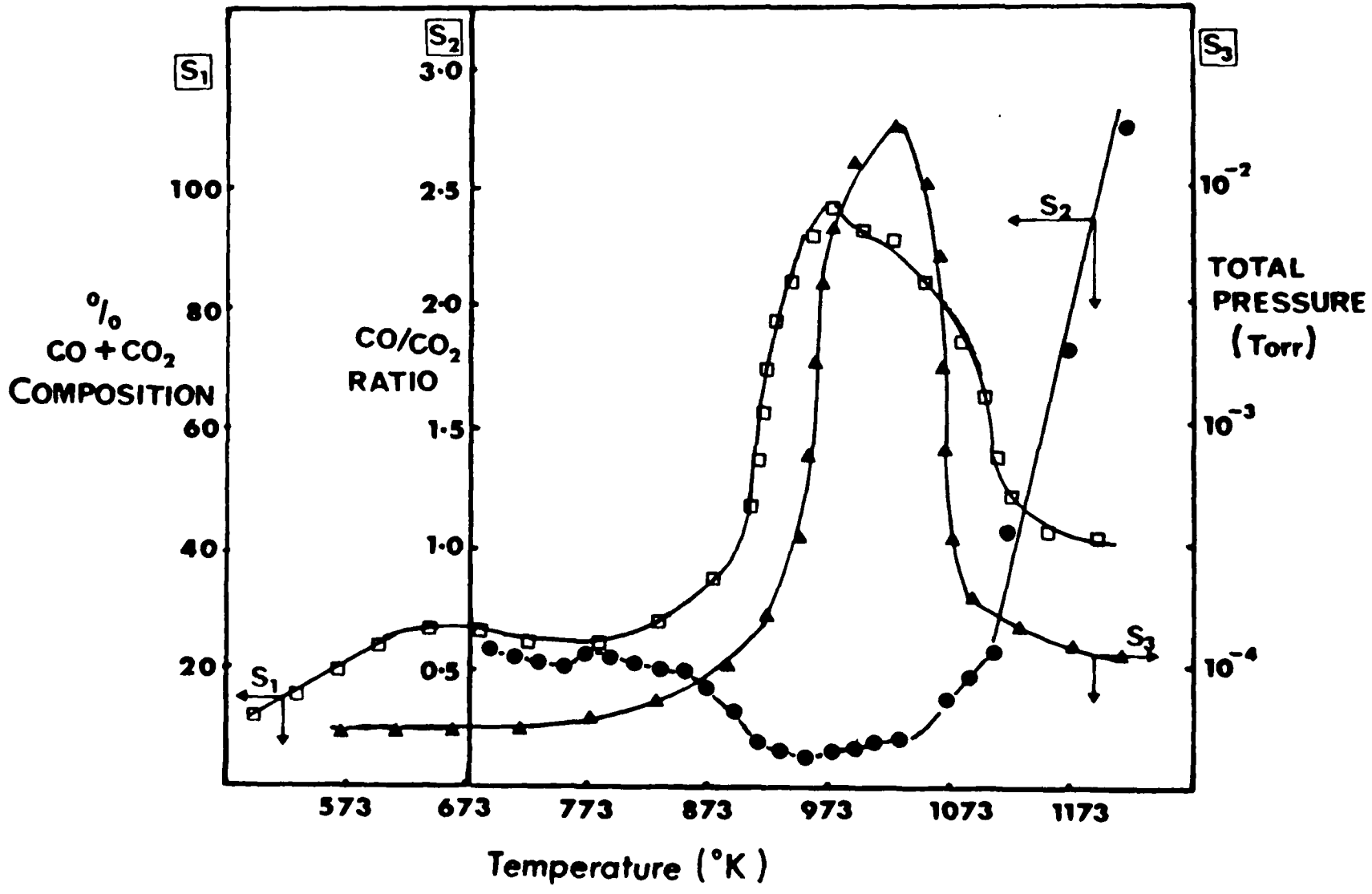
S1
S2
S3
100
80
60
40
20
3·0
2·5
2·0
1·5
1·0
0·5
10⁻²
10⁻³
10⁻⁴
% CO + CO₂ COMPOSITION
CO/CO₂ RATIO
TOTAL PRESSURE (Torr)
573
673
773
873
973
1073
1173
Temperature (°K)

Fig. 2

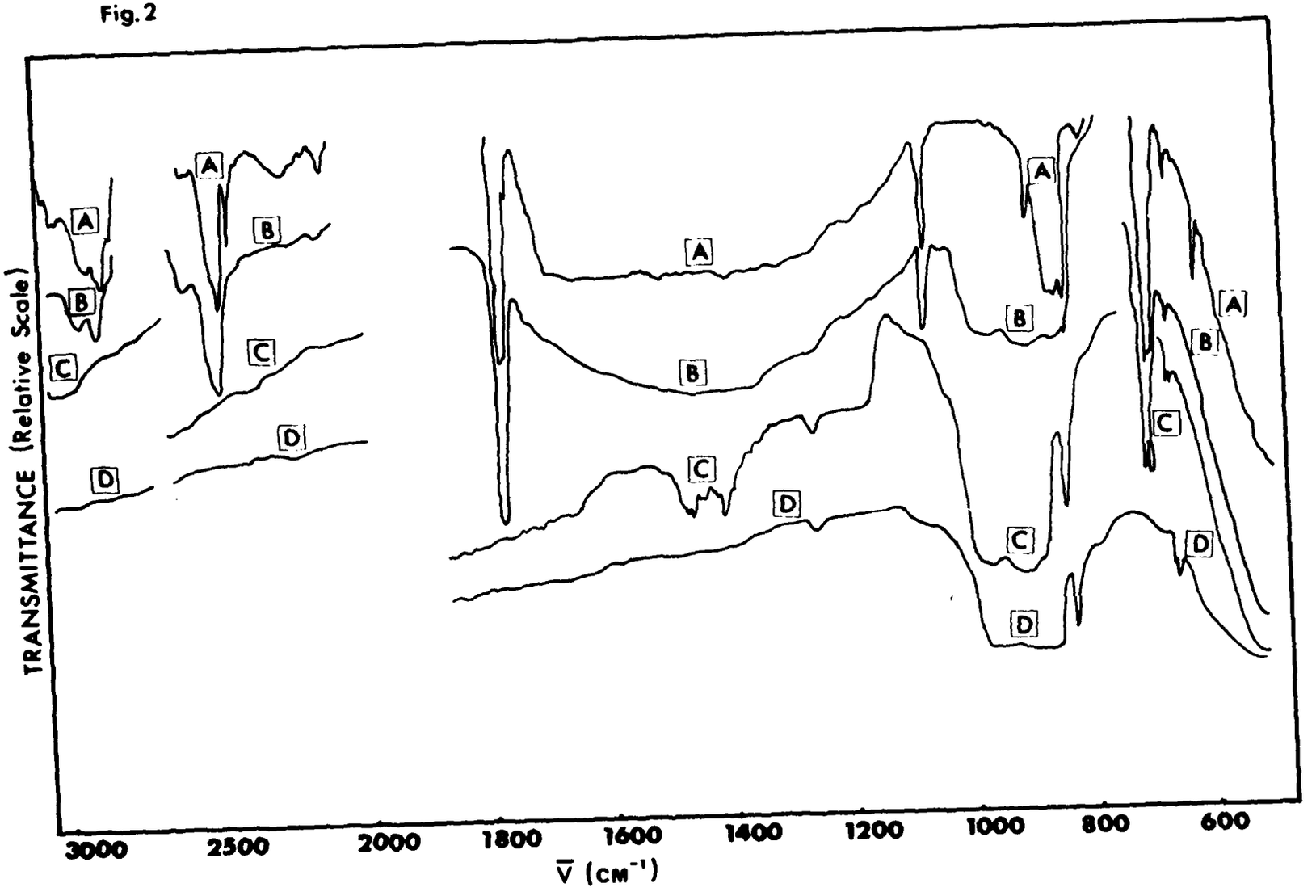
TRANSMITTANCE (Relative Scale)
A
B
C
D
3000
2500
2000
1800
1600
1400
1200
1000
800
600
$\bar{\nu}$ (cm^{-1})

Fig.3

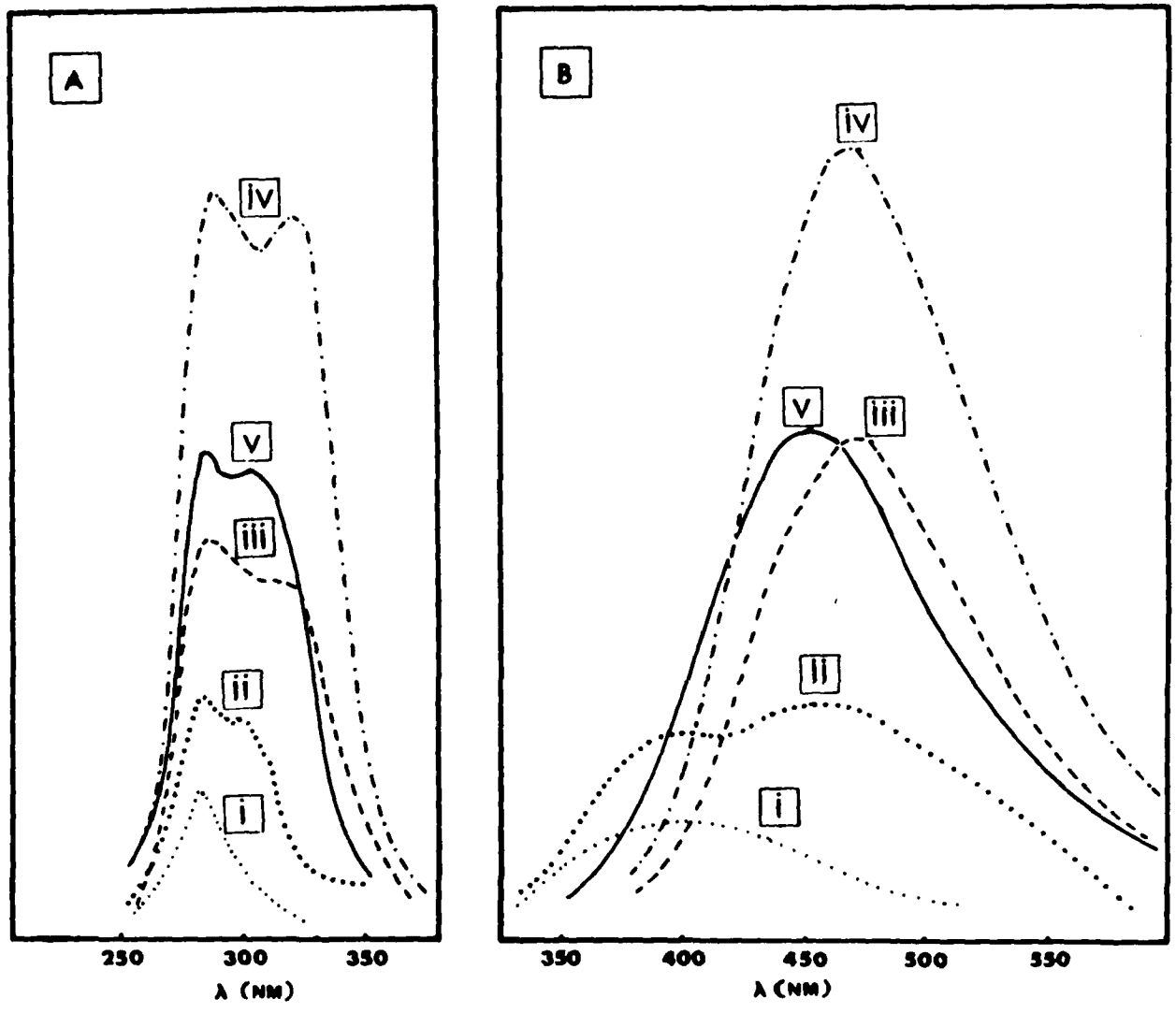
A
B
iv
v
iii
ii
i
INTENSITY
(ARBITRARY
UNITS)
250
300
350
λ (NM)
350
400
450
500
550
λ (NM)

Fig. 4

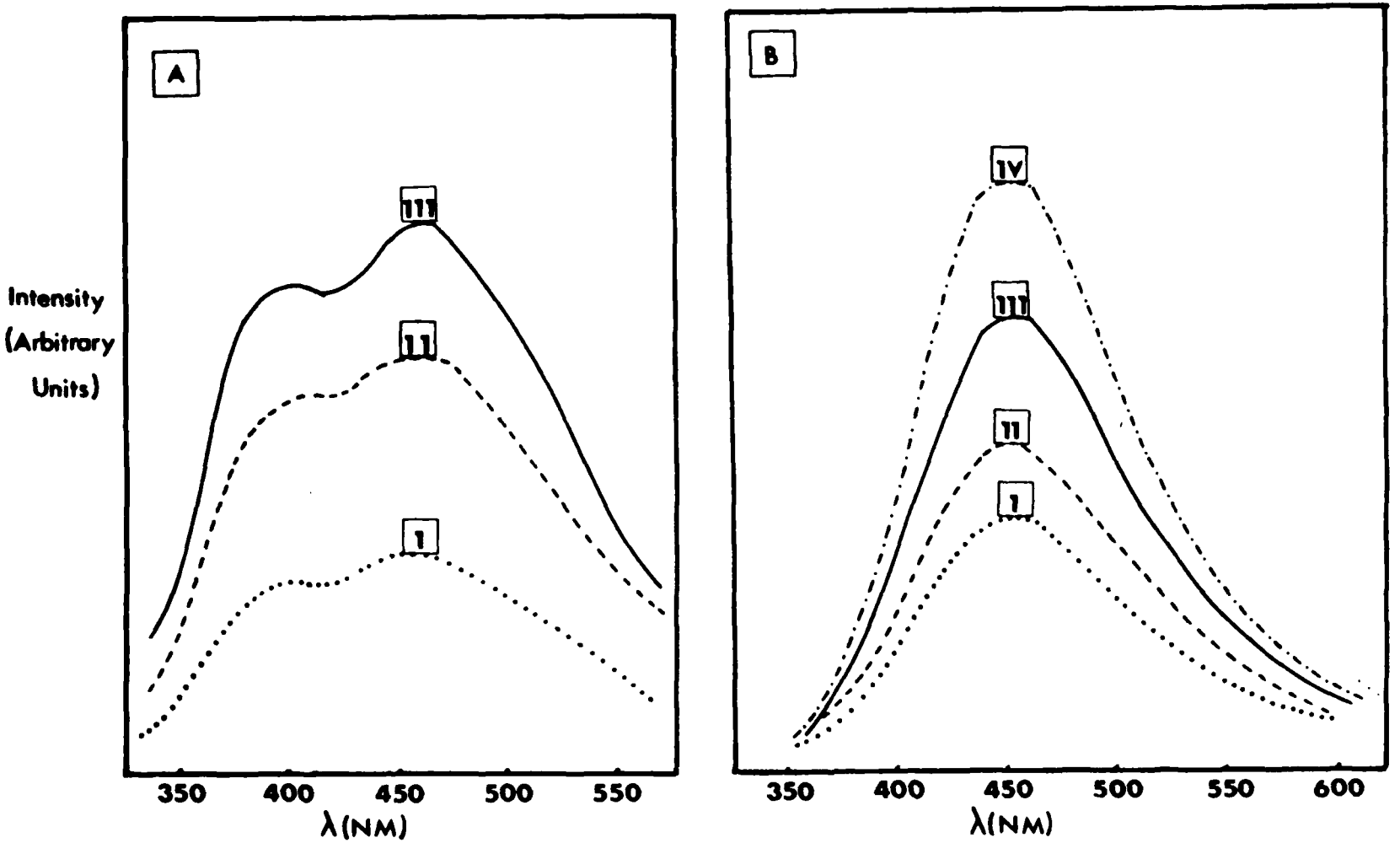
A
III
II
I
Intensity
(Arbitrary
Units)
350
400
450
500
550
λ(NM)
B
IV
III
II
I
350
400
450
500
550
600
λ(NM)

Fig.5A

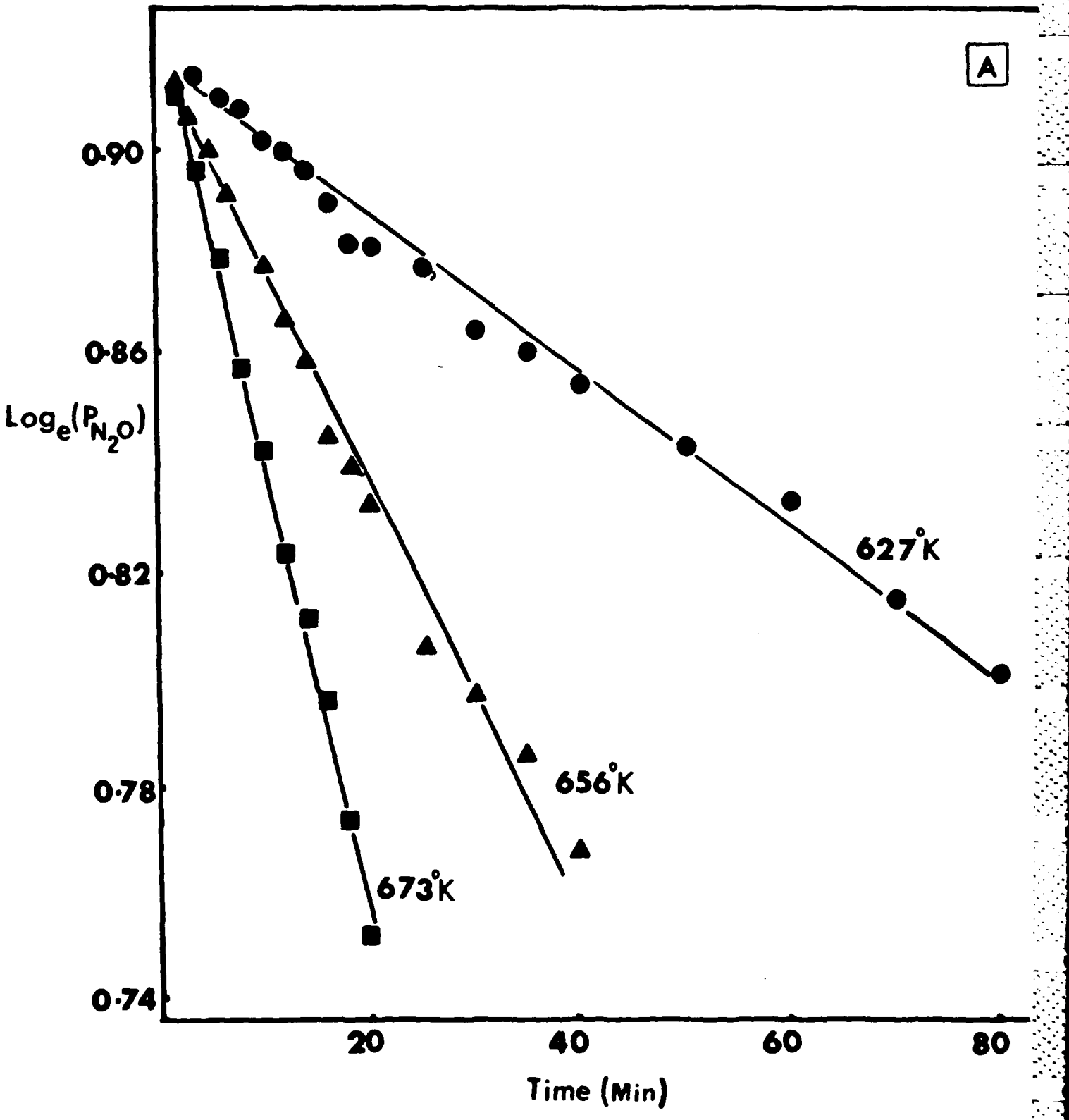
A
0·90
0·86
0·82
0·78
0·74
$Log_e(P_{N_2O})$
627°K
656°K
673°K
20
40
60
80
Time (Min)

Fig.5 B

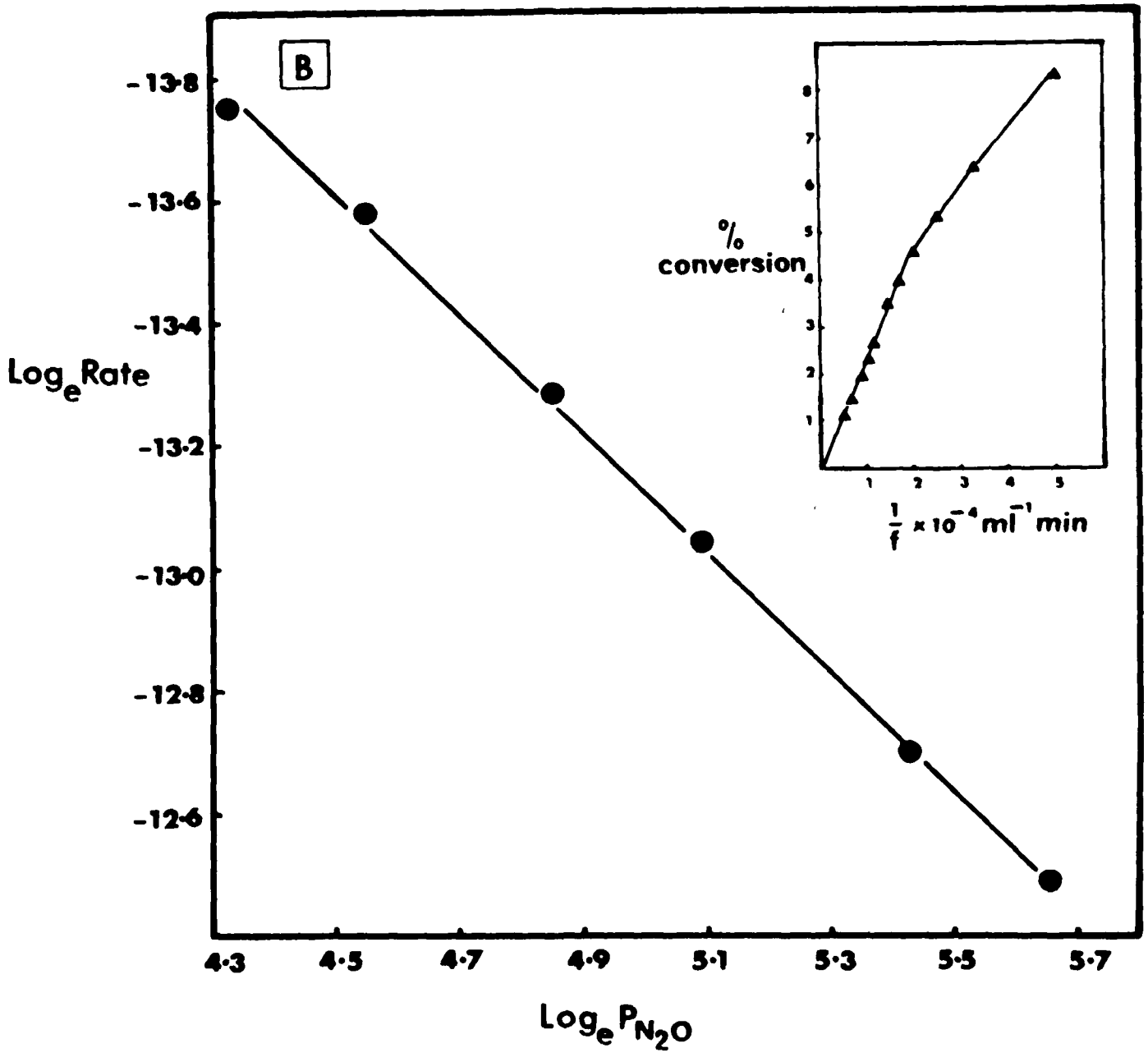
B
-13·8
-13·6
-13·4
-13·2
-13·0
-12·8
-12·6
Log$_e$Rate
4·3
4·5
4·7
4·9
5·1
5·3
5·5
5·7
Log$_e$P$_{N_2O}$
% conversion
1
2
3
4
5
6
7
8
$\frac{1}{f} \times 10^{-4}$ ml^{-1} min

Fig.6

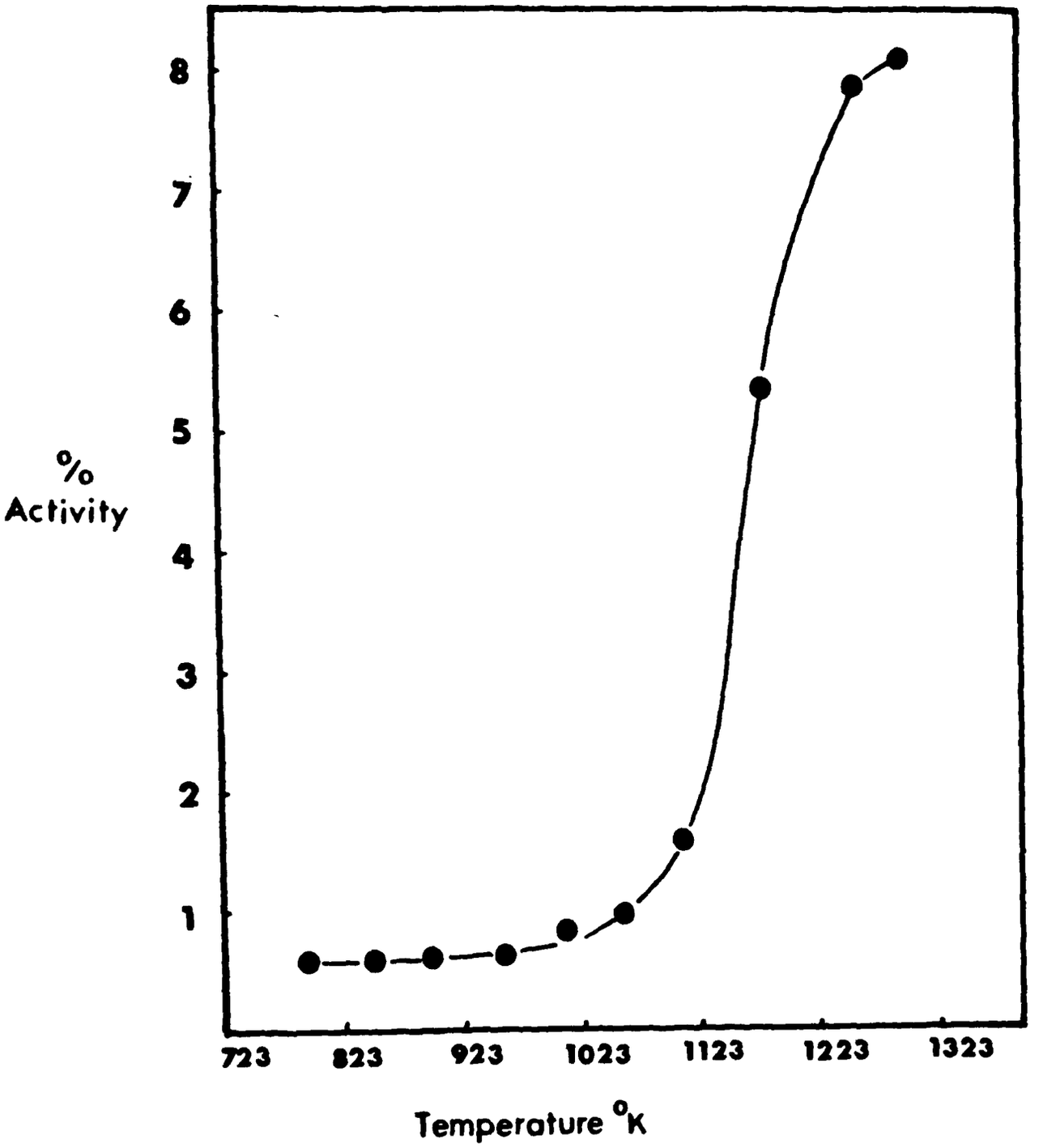
8
7
6
5
4
3
2
1
% Activity
723
823
923
1023
1123
1223
1323
Temperature °K

Fig.7

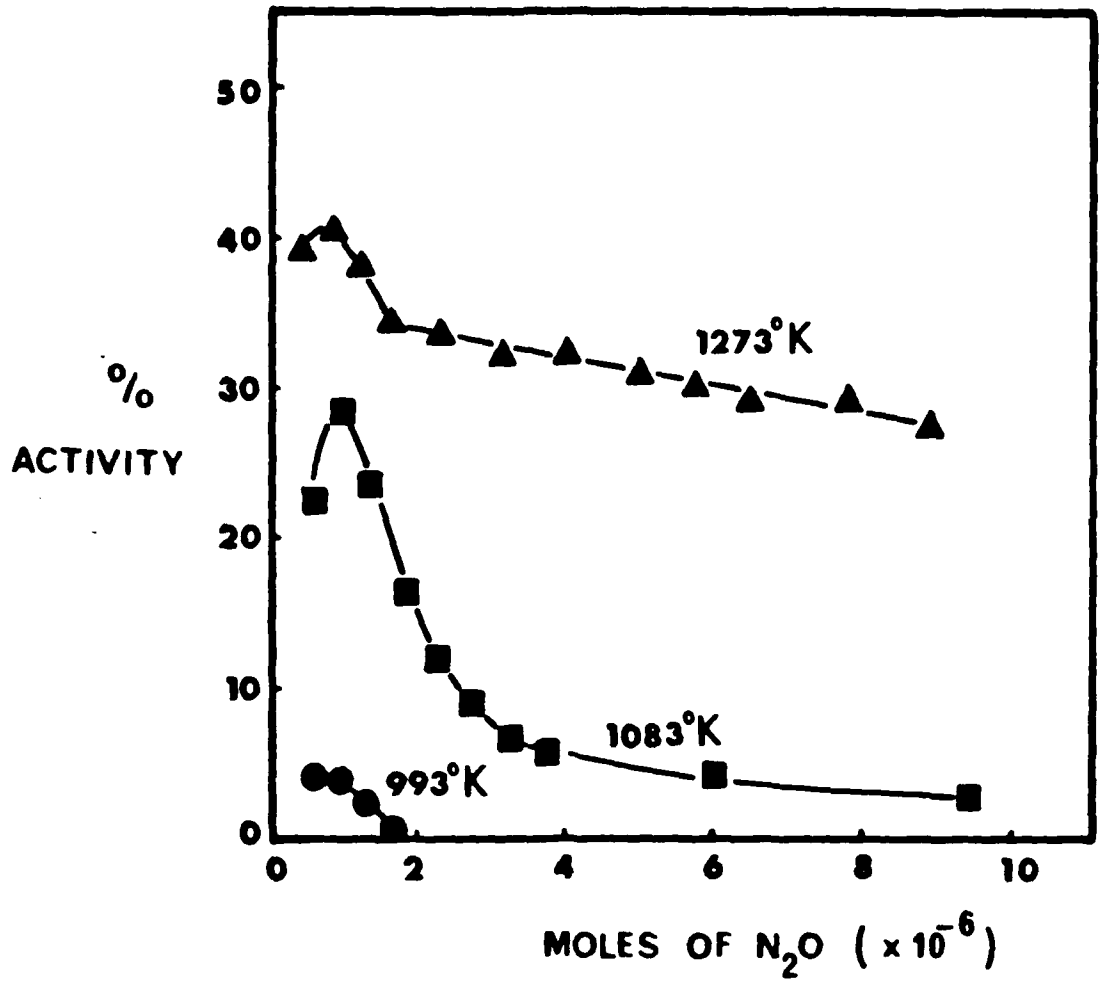
50
40
30
20
10
0
% ACTIVITY
1273°K
1083°K
993°K
0
2
4
6
8
10
MOLES OF N_2O ($\times 10^{-6}$)

Fig.8

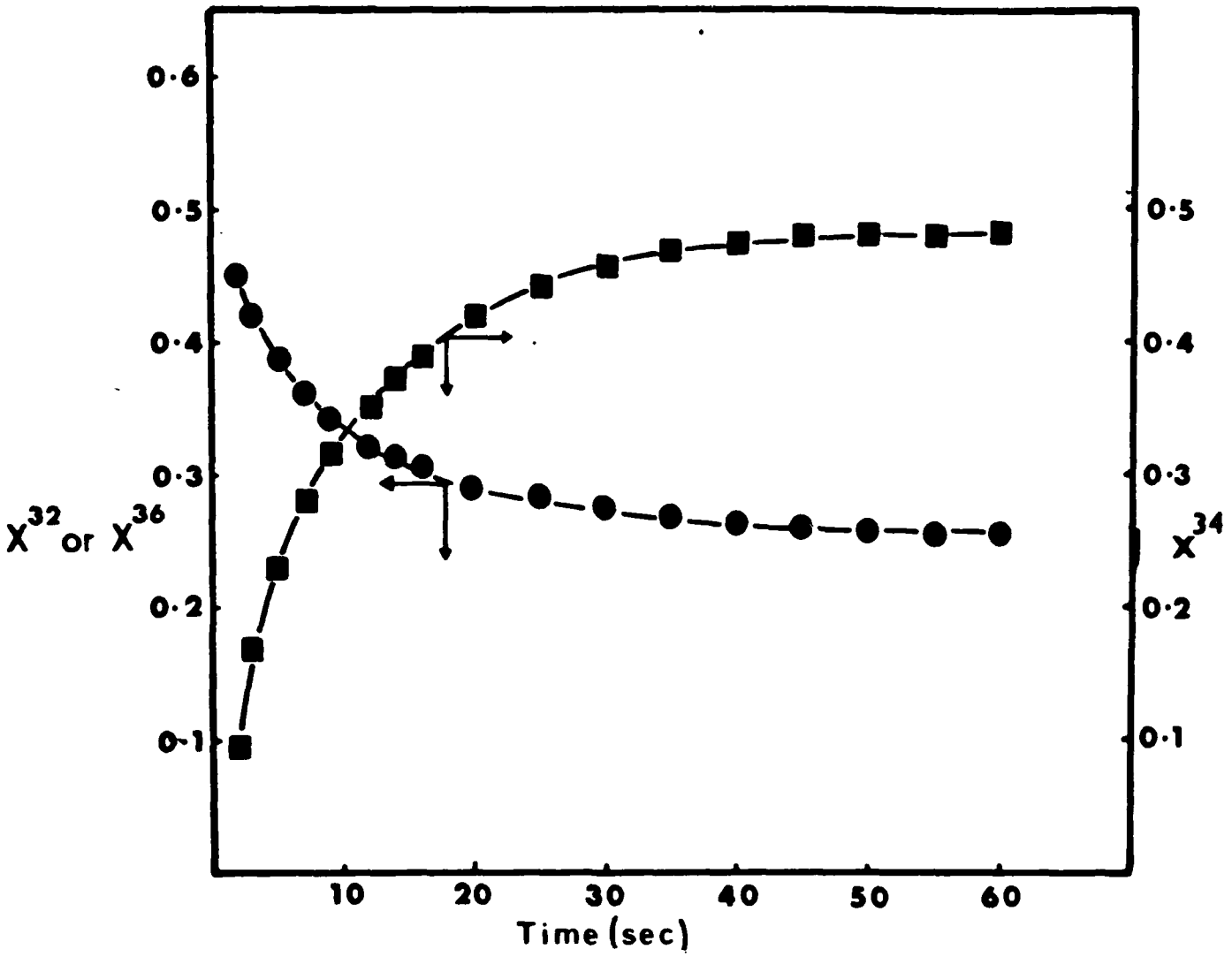

Fig.9

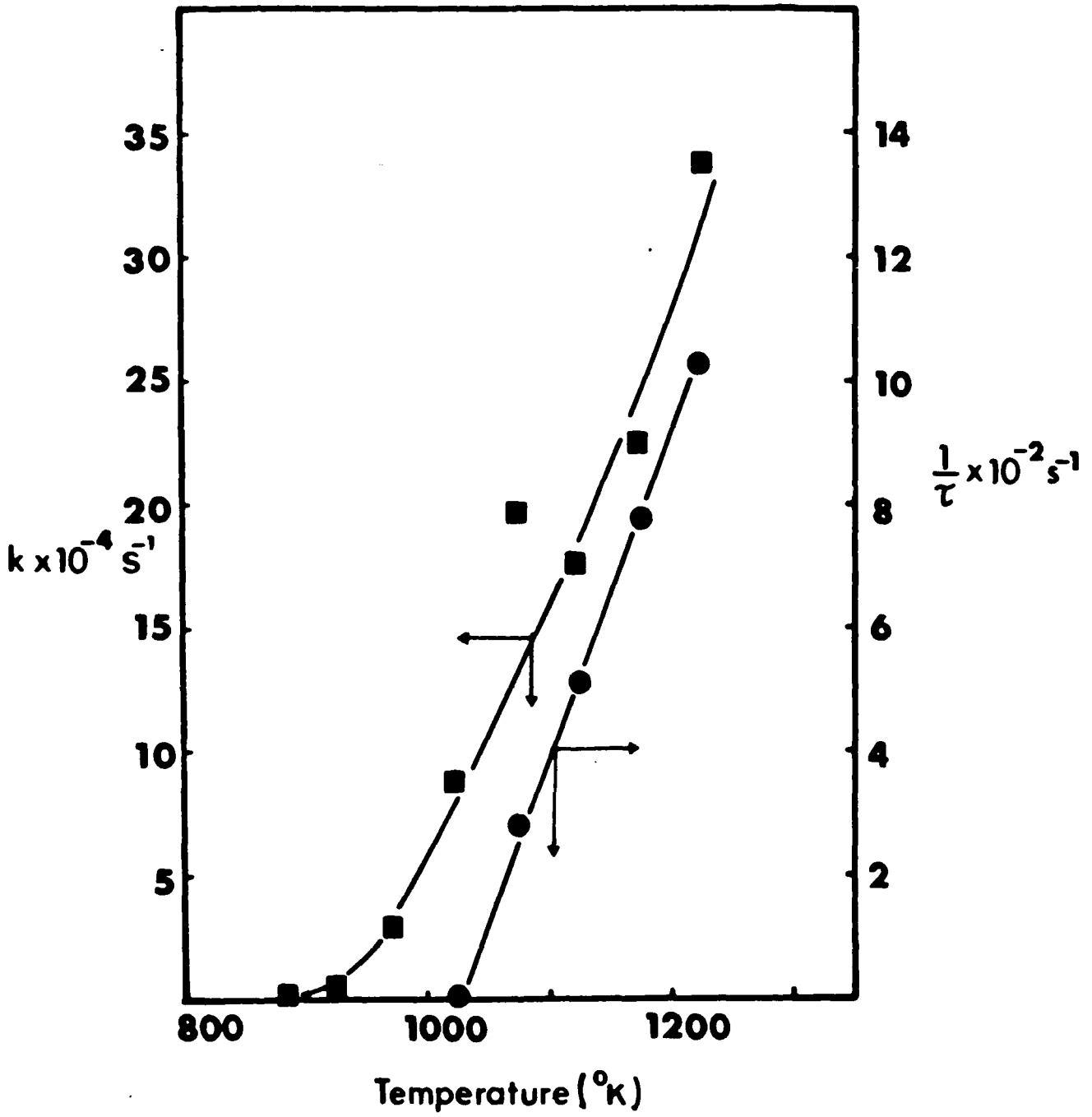
35
30
25
20
15
10
5
k x10⁻⁴ s⁻¹
14
12
10
8
6
4
2
1/τ x10⁻² s⁻¹
800
1000
1200
Temperature (°K)

END

FILMED

12-85

DTIC